Dear Editor,

First of all, we would like to thank the reviewers for their comments and suggestions which have been really useful to improve our work.

The corrections suggested by both reviewers, listed in chronological order, have been applied as here reported (you will find our answers in blue):

Anonymous Referee #2 (Received and published: 2 November 2017)

General Comments: The authors found a strong disagreement of Rn based CH_4 flux estimates with the values in the EDGAR inventory. Potential reasons for this should be discussed in more detail. What is the contribution in the regional EDGAR CH_4 emissions from different source sectors, e.g. enteric fermentation? Which sector seems to be the main cause for the disagreement? Discussing such questions would allow for inventory people to better learn from such observationally based estimates.

Thank you for highlighting this point. Given that the EDGAR CH_4 emissions are provided on an annual scale, we would like to underline the fact that the main aim of this work is to show how Rn-based CH_4 flux estimates can offer information on 'seasonal sources'. These can be anthropogenic sources too, but with seasonal behaviour (e.g. agricultural activity), which are not captured in EDGAR or classical UNFCCC inventories. Although we observed that annual mean Rn-based CH_4 flux estimates are lower than the values based on the EDGAR inventory over the study period, we were much more interested in understanding possible reasons for the relative increase and/or decrease of these differences during two semesters of the year (June-December and January-May) (Figures 9 and 11 of the manuscript).

In the results paragraph of our revised manuscript we have now commented on the possible reasons for the observed disagreement between the two methods and we have also carried out a second experiment using a comparison factor, coming from another 222Rn emission product, to rescale our results. We find that the disagreement with EDGAR is mainly reduced, while the seasonal amplitude of the RTM-based CH4 emissions is enhanced. The differences between Rn-based CH4 flux estimates and values based on the EDGAR inventory could be mainly due to:

1) applied RTM methodology:

A possible underestimation of the ^{222}Rn flux data used within the RTM. The outputs from the UHU radon flux model will lead to lower FR_CH_4 fluxes if they are lower than actual ^{222}Rn fluxes (Equation 2). Karstens et al., 2015 compared their radon flux model with UHU model and they found a generally 40 % higher^{222}Rn exhalation rate in their map than in the López-Coto et al. (2013) map. The 40% factor observed by Karstens et al., 2015 has been applied in our study to calculate rescaled FR_CH_4 values (FR_CH_4_rescale). In Figure 11 boxplot of the modified manuscript monthly medians of these values have been compared with FE_CH_4 and FR_CH_4 fluxes. FR_CH_4_rescale fluxes show a good agreement with FE_CH_4 fluxes during the months between June and December, when the transhumant livestock stays in the GIC3 area. A further validation of both 222Rn flux models should be carried out with high spatial resolution over Europe as suggested by Karstens et al., 2015.

2) Spatial and temporal disaggregation in EDGAR:

The mean contribution in the regional EDGAR CH_4 emission of the enteric fermentation is 38% of the total (EDGARv4.2, 2010). The spatial distribution of these emissions over the country in the EDGARV4.2 methodology (http://edgar.jrc.ec.europa.eu/methodology.php) was built up using spatial proxy datasets with the location of energy and manufacturing facilities, road networks, shipping routes, human and animal population density and agricultural land use, which vary over time. National sector totals are then distributed with the given percentages of the spatial proxies over the country's area. This could lead to the assignment of higher emissions in some regions such as the GIC3 area if transhumant cattle are fully taken into account.

The fact that the RTM and EDGAR results are in better agreement during the month when cattle are present could suggest that the inventory did attribute emissions there when scaling annual totals. Actually, The Unión de Pequeños Agricultores (UPA, 2009) reports that between 2004 and 2009 an average of 800,000 transhumant animals were hosted in Spain and 40,000 (5% of total) were counted in the province of Ávila (extension: 8050.15 km²) for an average of 5 cows per square km where the GIC3 station is located and their whereabouts can be expected to change local/regional CH_4 emissions when they are present/moving in a region.

3) Systematic/seasonal bias in footprint calculations

To estimate the impact of the EDGAR emissions for the GIC3 region, we rely on footprints calculated using ECMWF-FLEXPART. If the surface sensitivity calculated in the model is systematically biased (lower) compared to the real sensitivity, the FE_CH_4 fluxes could be underestimated. Even slight seasonal changes of model performance could be possible due to the fixed PBLH scheme (300m). If the true PBLH was below 300m during winter we would overestimate the impact of emissions as particles above the PBLH, but below 300m would still be assumed to be impacted by emissions. Another point to consider is that the night-time PBLH does not show strong seasonal change (see Figure 4b). The sudden increase in CH_4 emissions during the period when transhumant cattle reach the GIC3 regions cannot be explained by this, as the models ability to represent atmospheric conditions should not change from one week to another, given that general meteorological conditions do not change on this time-scale, see radon and met data in Grossi et al 2016. Finally, RTM and EDGAR methodologies are based on the same footprints so this effect should not influence the relative differences observed by Cattle and No-Cattle seasons.

Footprint calculation: What was used as the height below which particles are assumed to be influenced by surface fluxes? Ln 210 mentions 300 m, but what was assumed in cases with a nocturnal boundary layer height below 300 m? Particles above the top of the nocturnal boundary layer should not be influenced by surface fluxes. If the method assumes all particles below 300 m to be influenced by surface fluxes, the associated uncertainty in the footprint should be described. Note that usually there is strong wind shear near the top of the nocturnal boundary layer, which worsens a potential error in estimated footprint area.

We made the common assumption in FLEXPART of a fixed height layer to calculate the footprint or source-receptor relationship (e.g. Stohl et al. 1998, Pan et al. 2014). A PBLH cut-off of 300m was assumed for the calculation of the footprints using 24h back-trajectories and waiting for the particles to pass over the footprint (Equation 3 and 4 of the revised manuscript). Although this selection could introduce an error in the estimation of the residence time within the nocturnal boundary layer, this residence time is used to calculate both FE__CH_4 and the effective ^{222}Rn flux (used to calculate the FR_CH_4 fluxes, see equation 2 of the revised manuscript). In addition, night-time PBLH at GIC3 does not show strong seasonality (see Figure 4a in manuscript).

We have added this information in the methodology section and discussed its influence on the results in the discussion.

Also it is unclear how exactly the weighting function w(x,t) (Eq. 2) was normalized, and what the exact time limits in the summation in Eq. 2 are. This needs to be clearly described.

We have added this, as suggested (Equation 4).

Please use an equation to better illustrate the FLEXPART Radon-tracer method derived CH_4 fluxes (FR_CH4).

It has been added as suggested (Equation 2).

Rather than showing a somewhat hard to read map in Fig 1, why not show the footprint map and a map of the inventory based emissions? That would be better related to the rest of the manuscript.

Thanks for this suggestion. We have now added the footprint and EDGAR inventory maps (new Figures 1 and 2) within the manuscript and the map of the transhumance paths was moved to the supplement material (new Figure S2).

Specific comments

Ln 90: “flux in this area is of about” I suggest to drop the “of”

This has been changed.

Ln 124: “The instrument accuracy for CH_4 is of 0.36 ppb” I suggest to drop the “of”

This has been changed

Ln 143: Is the canopy really below 20 cm? May be this should read “below 20 m”?

Yes, it was 20m - thanks. This has been changed

Ln 157: Please rephrase the section header, and avoid unreadable terms (i.e. avoid underline characters).

This has been changed

Ln 177: For which time intervals was the correlation between CH_4 and Rn assessed, for a single night? This should be stated.

This was stated in Section 2.4.1 when the radon tracer methodology was presented. We have changed this sentence to clarify it.

Ln 231: replace “is” by “of”

This has been changed

Ln 242: drop “of”

This has been changed

Ln 243: “it is of 30 ppb” drop the “of”

It has been changed

Fig. 3 and Fig. 4: it would be useful to show the monthly boxplots also separately for day and night, especially for attributing changes in daily amplitudes; it could well be that low nocturnal PBLH drives the larger amplitude during summer rather than the deeper mixing during daytime as stated in Ln 293.

The additional results have been added and discussed in the results paragraph.

Figure 7: the legend is unnecessary, I suggest removing

This has been changed

Fig. 8: Why are not the monthly values of the UHU climatology shown? Also, it should be mentioned what “local flux” means; is it the UHU Rn flux value of the local pixel containing the GIC3 station?

Monthly UHU values are not shown in this plot because they were already shown in Figure 7. The local flux is actually the UHU Rn flux value of the local pixel containing the GIC3 station. This has been pointed out within the manuscript.

Ln 336: “is of” drop the “of”

This has been changed

Ln 336: Looking at the red circles in Fig. 9 it seems that the mean should be much lower, somewhere around 0.1 mg CH4 m-2 h-1.

The reviewer is right, there was an editing error. The value was 0.13 and this has been corrected.

Fig. 9: the grey shaded rectangles seem to be at the wrong position. In the figure caption, e.g. week 21-27 June 2014 is mentioned, while the rectangle seems to be at around mid-end of March 2014. Also, the green shaded rectangle (presence of animals) is located at times with low FR_CH4.

The reviewer is right, there was an error in the plot because the shaded boxes moved. This has been corrected.

Fig. 10: Please use simple numbers as x-axis labels to indicate the months.

This has been changed.

Ln 395-397: this is a repetition of Ln 287-289

We have deleted the repeated sentence.

Ln404-405: I disagree with the assumption that CH4 fluxes vary only to a small degree; this has not been shown. In Ln 390 the authors even argue that the hysteresis in Fig. 5 is due to changes in local emissions. I suggest citing literature describing the emissions from animals; what is expected from the process level, e.g. do ruminants emit constantly, or more during certain parts of their diurnal feeding cycle?

We have extended and improved this section in the discussion. We agree with the reviewer that the CH_4 fluxes can also vary on a diurnal cycle. The hysteresis observed in Figure 5 which could be due to changes in local emissions appears between 13.00-18.00 UTC, which cannot be tracked using the RTM. Although some studies have found strong diurnal changes in ruminant emissions, e.g. Bilek et al. 2001, Wang et al., 2015, these studies link the diurnal pattern of methane emissions to the ruminant feeding cycle in feedlots. They find that the feeding regime, feeding frequency and the amount of feed offered can alter methane emissions. Given that transhumant cattle are moved to the GIC3 region to graze, we would not assume that this effect is as pronounced as in feedlots, as cattle can feed more continuously at GIC3. Mohammed, et al. (2011) reported a fairly flat daily cycle of CH_4 emissions from grazing, especially if compared to aforementioned feedlot studies. However, we actually do not have any direct information about the feeding cycle of grazing Gredos livestock, but we now mention this as a future step in the identification of methane emission in this area in the discussion.

Anonymous Referee #1 (Received and published: 2 February 2018)

The text is written clearly enough, but should be further improved - best revised by a native speaker/writer (e.g. to improve the structure of sentences).

Thanks, the text has now been corrected by a native English writer.

Figures 1 to 3 are too small and the legends as well as labels of Figs. 1 to 2 are not legible

Figure 1 has been deleted and Figure 2 has been moved to the supplement, as suggested by referee #2.

Figure 2S is much too crowded with labels and not well legible.

Figure 2S, now 4S, has been changed as suggested.

I am not convinced by the color scale used in figures 5 to 7; is this safe for color-blind readers? Particularly in Fig. 5, the colors for hours 5 to 8 look practically the same.

We have tried to make the plot acceptable for all color-blind readers but we finally decided to use the first version of the plot because the whole paper has colored figures. We have avoided green as most colorblindness falls on the green-red spectrum (deuteranopia).

I agree with the comment by Referee #2 regarding the disagreement of 222Rn-based CH4 flux estimates with the EDGAR inventory-based ones. While it might well be that livestock is responsible at least for a part of the CH4 signal, I failed to see a proof in this work.

The possible reasons for this disagreement have been added in the discussion and a detailed explanation has been given above (reply to Referee #2).

Moreover, EDGAR should be sensitive to livestock emissions (as they are non-natural), but the opposite seems to be the case. This seems to indicate that the main processes driving CH4 variability at GIC3 area are natural ones or that EDGAR is performing poorly at least when livestock is concerned. In my opinion, the focus, discussion and conclusions of the article should be more on the method and less trying to link the CH4 variability mostly to livestock as it is the case in the current version. In this context, I also find the title of the article a bit ill chosen.

Our interpretation of the findings is not that EDGAR performs poorly for the livestock component, as the different methods are in reasonable agreement during the period when livestock is present in the GIC3 region mainly using the RTM_CH4_rescale. Our results seem to show that the RTM-based CH4 fluxes decrease during the period without transhumant livestock in the GIC3 area and they increase during June-December when the livestock is back to the region. On the contrary, the EDGAR based CH4 fluxes do not show any seasonality. Thus, it seems more likely that all (annual) CH4 emissions of these cattle have been attributed to this region, although they are physically moved to different regions. Given the scope of EDGAR we would not expect it to cover all local processes and this study intends to help identify transhumance as a potential issue that could be improved (added) in future emission inventories for this region and Spain as a whole. However, we agree with the reviewer that the conclusions of our work should be more focused on the applied method and the paragraph has been changed accordingly. The title of the article has been changed to better fit with the work done

The section 2.2 is very minimalistic. I acknowledge that concise descriptions of measurement systems is not in the scope of articles in ACP, but as there is no other reference to direct the reader to, at least a schematic of the measurement setup could be added in the Supplement.

In agreement with the reviewer's suggestion, a schematic diagram of the measurement set-up used at the GIC3 station has been added as Figure S3 in the supplement.

Specific comments and technical corrections

Note on Technical corrections: in some cases, I have marked a word or formatting only once, but make sure to apply the corrections throughout the text where relevant.

Line 17 (L 17): instead of "concentration" use rather "(dry air) mixing ratio". Sentence is too long and difficult to read/understand.

The sentence has been changed as, suggested by the reviewer.

L 21: delete "previous" done

L 27: delete "of" in "is of 0.32" done

L 36: reported by whom? 'by each country' has been added

L 49: "....data and data products..." done

L 51: "In some European regions...." done

L 52: what do you mean by "remote"? Please define this more clearly. This has been changed to 'with stations located in natural parks'

L 64: "In this study, we analyzed the time series.....and December 2015." this has been changed

L 68: delete "Particularly," done

L 69: delete "such as Extremadura" – you mention it in L 72 again. done

L 75: delete "further"; better replace "mobile" with "ephemeral" or "transient" (without the quotes in the text) done

L 83-85: are the durations of the cold and warm seasons defined anywhere in the text? This has been done now.

L 91: "The GNP is located in a granitic basement;"? Rather: "The GNP has a (predominantly) granitic basement and is thus covered by granitic soils with high ...." Fig. 1: missing unit in the legend, add reference for CORINE/the map (...., 2007)

This has been changed

L 98: delete "Particularly," done

L 100: "In Figure 2, a map ..." done

Fig. 2: instead of "Source", use "Modified from" done

L 120: the reference "Crosson, 2008" is not well chosen here – it would be better to leave it out. Change to "... measured with a frequency ....using a..."

done

L 125: a target gas is, more precisely, used for “checking the stability and quality of the instrument calibration”. Please define better what you mean by “according to the definitions of the World Meteorological Organization (WMO).”; add a reference.

A definition and appropriate reference have been added

L 131: “...of both ARMON and G2301 analyzer are...” done

L 134: Sample air drying system done

L 144: “...area is quite hilly.” is not very explicit, please elaborate on this. A figure showing the terrain would be helpful for understanding to what extent it is justified to apply a method as RTM at GIC3 (c.f. assumptions in Lines 160 to 175).

A figure showing the GIC3 topography has been added as Figure S1 in the supplement.

L149: how representative are the ECMWF PBLH data for the GIC3 site? This question also relates to previous comment (L 144) – is the variability of the terrain captured well enough in the ECMWF model?

Seidel et al., 2012 found that compared with radiosonde observations, both the re-analysis and the climate models produce deeper layers due to the difficulty in simulating stable conditions. In vertical profiles they introduce height uncertainties that can exceed 50% for shallow boundary layers (<1 km), but are generally <20% for deeper boundary layers. This information has been added to the revised manuscript.

L 185: please explain the acronym UHU - done

L 195: “...country on a spatial grid.”- done

L 196: provides global annual CH4 emissions on a 0.1 degree resolution - done

L 225: “...sample system 11 % of the...” How are the data gaps distributed; evenly or was there a concentration of data gaps in some periods /in which ones? This information has been added. We mainly missed summer 2013.

Fig. 3 I presume “Hour of the day” is in UTC? Please add. Also, better use nmol/mol instead of concentration, which should only be used in communicating with the general public (see e.g. GAW Report No. 229). - done

L245: I cannot follow this sentence “A light increase of methane concentrations seems to be observed between the first and the second semester of the year.” – please clarify. This has been clarified in the manuscript

L 305: delete “Indeed,” - done

Fig. 9: correct the month name abbreviations to English language; green circles are poorly visible - done

L 392: if CH4-enhanced air masses were transported in the afternoon, would we not see the same pattern for Rn as well? Please elaborate on this in more detail. It would be interesting to actually see a typical footprint for such events.

If air masses rich in methane, but not in radon, are transported to the station, we will not be able to see the same daily pattern in radon concentration. We have tried to explain this effect now within the manuscript using Figures 9, 10 and S4 of the supplement, where an increase of the methane fluxes when air masses are coming from the Madrid direction is shown.

L410: There was not much said on the landscape, precipitation patterns, water (bodies), etc. in the region – it is a reasonable guess that livestock has something to do with it, but there might be other reasons for this increase in CH_4 fluxes - this should be discussed

We have added this in the conclusions paragraph.

Study of the ~~main processes driving~~daily and seasonal atmospheric CH_4 mixing ratio variability in a rural Spanish region using ^{222}Rn tracer

~~C.~~Claudia Grossi[a,1], ~~F.~~[2], Felix R. Vogel[b], ~~R.~~Roger Curcoll[a,2]~~, I. López-Coto~~[c,3], ~~A.~~Alba Àgueda[a,4], ~~A. Vargas~~[d]~~, X.~~Arturo Vargas[c], Xavier Rodó[a,~~e~~d,3,5]~~, J. A.~~ Josep-Anton Morguí[a,~~f,2~~e,3]

[a] Institut Català de Ciències del Clima (IC3), Barcelona, Spain

~~*[b] Laboratoire des Sciences du Climat et l'Environnement (LSCE-IPSL), CEA-CNRS-UVSQ, Université Paris-Saclay, Gif-sur-Yvette, France*~~

~~*[c] Departamento de Física, Universidad de Huelva (UHU), Spain*~~

[~~d~~b] Climate Research Division, Environment and Climate Change Canada, Toronto, Canada

[c] Institut de Tècniques Energètiques (INTE), Universitat Politècnica de Catalunya (UPC), Barcelona, Spain

[~~e~~] ~~Institució~~[d] Institució Catalana de Recerca i Estudis Avançats (ICREA), Barcelona, Spain

[~~f~~e] Departament ~~d'Ecologia~~Biologia Evolutiva, Ecologia i Ciències Ambientals, Universitat de Barcelona (UB), Barcelona, Spain

Present addresses:

[1] Institut de Tècniques Energètiques (INTE), Universitat Politècnica de Catalunya (UPC), Barcelona, Spain

~~[2] Institut~~[2] Physics Department, Universitat Politècnica de Catalunya (UPC), Barcelona, Spain

[3]Institut de Ciència i Tecnologia Ambientals (ICTA), Universitat Autònoma de Barcelona (UAB), Cerdanyola del Vallès, Spain

~~*[3] National Institute of Standards and Technology (NIST), Gaithersburg, MD, US*~~

[4] ~~Centre~~[4]Centre d'Estudis del Risc Tecnològic, Universitat Politècnica de Catalunya (UPC) - BarcelonaTech, Barcelona, Spain

[5] CLIMA2, Climate and Health Program, ISGlobal (Barcelona Institute of Global Health), Barcelona, Spain

Correspondence to: Claudia Grossi (claudia.grossi@upc.edu), Felix Vogel (felix.vogel@~~lsce.ipsl.fr~~canada.ca)

Abstract. ~~Atmospheric concentrations of the two main greenhouse gases (GHGs),~~ The ClimaDat station at Gredos (GIC3) has been continuously measuring atmospheric (dry air) mixing ratios of carbon dioxide (CO_2) and methane (CH_4), ~~are continuously measured since November 2012 at the Spanish rural station of Gredos (GIC3), within the climate network ClimaDat, together with atmospheric radon (^{222}Rn) tracer and~~ as well as meteorological parameters~~. The~~ , since November 2012 . In this study we investigate the

Style Definition: ...

Formatted: Left: 3 cm, Right: 3 cm, Top: 2.5 cm, Bottom: 2.5 cm, Height: 29.7 cm

Formatted: Font: 10 pt, English (U.S.)

Formatted ...

Formatted ...

Formatted ...

Formatted: Font: Italic, Spanish (International Sort), Superscript

Formatted: Font: Italic, Spanish (International Sort)

Formatted: Font: Italic, Spanish (International Sort), Superscript

Formatted: Font: Italic, French (Canada), Superscript

Formatted ...

Formatted ...

Formatted ...

Formatted ...

Formatted: Footer, Right

atmospheric variability of CH_4 ~~concentrations measured from~~mixing ratios between 2013 ~~to~~and 2015 at GIC3 ~~has been analyzed in this study. It is interpreted in regard to the variability of measured atmospheric~~with the help of co-located observations of ^{222}Rn concentrations, modelled ^{222}Rn fluxes and modelled ~~heights of the~~ planetary boundary layer heights (PBLH~~) for the same period. In addition, nocturnal fluxes of CH_4 were estimated using two methods: the Radon Tracer Method (RTM) and one based on the application of the EDGARv4.2 bottom-up emission inventory.~~). Both ~~previous methods have been applied using the same footprints, calculated by the atmospheric transport model FLEXPARTv6.2.~~

~~Results show that~~ daily and seasonal changes in atmospheric CH_4 can be better understood with the help of atmospheric concentrations of ^{222}Rn (and ~~its~~the corresponding fluxes~~) can help to understand the atmospheric CH_4 variability.~~). On a daily ~~basis~~timescale, the variation in the PBLH ~~mainly drives changes in~~is the main driver for ^{222}Rn and CH_4 ~~concentrations~~variability while, on monthly ~~basis~~timescales, their atmospheric variability seems to ~~be due to~~depend on emission changes~~ in their~~. To understand (changing) CH_4 emissions~~. Median~~, nocturnal fluxes of CH_4 were estimated using two methods: the Radon Tracer Method (RTM) and a method based on the EDGARv4.2 bottom-up emission inventory using FLEXPARTv9.0.2 footprints. The mean value of RTM~~–~~-based methane fluxes (~~FLEXPART_RTM~~FR_CH_4) is 0.~~10~~11 mg CH_4 m^{-2} h^{-1} with a standard deviation of 0.09 mg CH_4 m^{-2} h^{-1}~~. Median~~ or 0.29 mg CH_4 m^{-2} h^{-1} with a standard deviation of 0.23 mg CH_4 m^{-2} h^{-1} when using a rescaled ^{222}Rn map (FR_CH_4_rescale). For our observational period, the mean value of methane fluxes based on the bottom-up inventory (~~FLEXPART-EDGAR~~FE_CH_4) is ~~of~~ 0.~~32~~33 mg CH_4 m^{-2} h^{-1} with a standard deviation of 0.08 mg CH_4 m^{-2} h^{-1}. ~~The FLEXPART_EDGAR_~~Monthly CH_4 fluxes ~~due to the contribution of the cities in the GIC3 region present a median value of 0 mg CH_4 m^{-2} h^{-1} with a standard deviation of 0.06 mg CH_4 m^{-2} h^{-1}. Monthly FLEXPART_RTM_CH_4 flux shows~~ based on RTM (both FR_CH_4 and FR_CH_4_rescale) show a seasonality which is not observed ~~in the~~for monthly ~~FLEXPART_EDGAR_CH_4 flux. Actually, a minimum during~~FE_CH_4 fluxes. During January-May~~ and a maximum~~, RTM-based CH_4 fluxes present mean values 25% lower than during June-December~~ are observed in these first fluxes. ~~. This ~~previous variability seems to be mainly related to the alternate presence~~seasonal increase of methane fluxes calculated by RTM for the GIC3 area appears to coincide with the arrival of transhumant livestock ~~in the GIC3 area. The results obtained in this study should be further investigated using longer CH_4 and ^{222}Rn time series to obtain more robust statistics and help to improve the seasonality of the emission factors from bottom-up inventories~~at GIC3 in the second semester of the year.

Formatted: Tab stops: Not at 1.62 cm + 3.23 cm + 4.85 cm + 6.46 cm + 8.08 cm + 9.69 cm + 11.31 cm + 12.92 cm + 14.54 cm + 16.16 cm + 17.77 cm + 19.39 cm + 21 cm + 22.62 cm + 24.23 cm + 25.85 cm

Keywords: methane, flux, radon, atmosphere, livestock, EDGAR, FLEXPART.

Introduction

The ~~importance~~impact of the atmospheric increase of ~~the~~ greenhouse gases (GHGs) ~~for~~on climate change ~~processes~~ is well known (IPCC, 2013).~~ Therefore,~~ GHGs emissions, due to natural as well as anthropogenic sources, are currently estimated and reported by each national agency to the United Nations Framework Convention on Climate Change (~~UNFCC~~UNFCCC). A ~~good~~better understanding of the underlying processes causing ~~the~~these emissions can help in the implementation of future emission reduction strategies. ~~Among the GHGs covered under the UNFCCC framework methane~~Methane (CH_4) is the second most important anthropogenic GHG~~,~~ that is covered by the UNFCCC. The atmospheric ~~concentration~~mixing ratio of CH_4 has substantially changed since pre-industrial times from a global average of 715 ~~ppb~~nmol mol^{-1} to more than 1774 ~~ppb~~nmol mol^{-1} (IPCC, 2013). ~~Today~~Nowadays, the contribution of CH_4 related to anthropogenic activities in the atmosphere represents about 25% of ~~the~~ total additional anthropogenic radiative forcing (IPCC, 2013). However, CH_4 has a relatively short lifetime in the atmosphere (~ 9 years) and this makes it relevant ~~for~~in defining immediate and efficient emission reduction ~~measures~~strategies (Prinn et al., 2000). Particularly~~,~~ in Spain, man-made methane emissions are mainly due to enteric fermentation (~~31~~38%), management of manure (20%), and landfills (36%) (WWF, 2014; MMA, 2016). The remaining methane contributions in Spain are due to rice cultivation (e.g. Àgueda et al., 2017), coal mining, leaks in natural gas ~~infrastructure~~infrastructures and waste water treatment~~-related processes~~. The CH_4 emission due to enteric fermentation related to livestock is directly linked to the number of animals of each type/breed of cattle, their age, their diet and environmental conditions (MMA, 2016). Spanish CH_4 emissions ~~for 2014~~ due to enteric fermentation were estimated to be ~~of~~ 11,704 Gg $CO_2$$^{-eq}$ (MMA, 2016).

In order to estimate GHGs emissions, bottom-up (based on fuel consumption and anthropogenic activity data) and top-down methods (based on atmospheric observations and modelling) are both widely applied and the scientific community ~~is focusing~~has focussed on reducing their related uncertainties and understanding systematic inconsistencies (e.g. Vermeulen et al., 2006; Bergamaschi et al., 2010; NRC, 2010; Jeong et al., 2013; Hiller et al., 2014). Top-down methods usually require both high-quality and long-term GHGs observations. European projects, such as InGOS (www.ingos-infrastructure.eu), and infrastructures, such as ICOS (www.icos-infrastructure.eu), aim to offer atmospheric CO_2 and non-CO_2 GHGs data and data products to better understand ~~GHG~~GHGs fluxes in Europe and adjacent regions.

~~Nevertheless~~Unfortunately, in ~~southern~~some European regions, such as Spain, there is still a significant lack of high-quality atmospheric GHGs observations. The Catalan Institute of Climate Sciences (IC3) has been working since 2010 within the ClimaDat project ~~at the creation of~~in setting up a network of ~~remote~~ stations in national parks for continuous measurements of mixing ratios of GHGs, tracers and meteorological parameters (www.climadat.es). The IC3 network mainly aims to monitor and study the exchange of GHGs between the land surface and the lower atmosphere (troposphere) in different ecosystems, which are characterized by different biogenic and anthropogenic processes, under different synoptic conditions.

Besides GHGs ~~concentrations~~mixing ratios, co-located observations of additional gases can provide us with useful tracers for source apportionment studies or to help us to better understand atmospheric processes (e.g. Zahorowski et al., 2004). ~~Particularly the~~The radioactive noble gas radon (^{222}Rn), due to its chemical and physical characteristic (e.g. Nazaroff and Nero, 1988), is being extensively used for studying atmosphere dynamics, such as boundary layer evolution~~,~~ (e.g. Galmarini, 2006, Vinuesa and

Formatted: Superscript

Formatted: Font: 10 pt, English (U.S.)

Formatted: English (U.S.)

Formatted: Normal (Web), Justified, Line spacing: 1.5 lines

Formatted: Internet Link, Font: 12 pt

Formatted: Font: 10 pt, English (U.K.)

Formatted: Font: 10 pt, English (U.K.)

Formatted: Footer, Right

Galmarini, 2007), and soil-atmosphere exchanges (e.g. Schery et al., 1998; Zahorowski et al., 2004; Szegvary et al., 2009; Grossi et al., 2012; Vargas et al., 2015; Grossi et al., 2016). European GHGs monitoring infrastructures ~~are~~ already ~~including~~include atmospheric ^{222}Rn monitors in their stations (e.g. Arnold et al., 2010; Zimnoch et al., 2014; Schmithüsen et al., 2016). The co-evolution of atmospheric ^{222}Rn and GHGs concentrations can also be used ~~in~~within the Radon Tracer Method (RTM) to estimate local/regional GHGs fluxes (e.g. Van der Laan et al., 2010; Levin et al. 2011; Vogel et al. 2012; Wada et al., 2013; Grossi et al., 2014).

Formatted: Font: 10 pt, English (U.K.)

In this study we analysed the ~~new~~ time series of atmospheric CH_4 ~~concentrations~~mixing ratios measured at the IC3 station ~~of~~in Gredos and Iruelas (GIC3) between January 2013 and December 2015 ~~has been analyzed.~~. The main aim was to investigate the ~~major causes influencing~~main drivers that influence the daily and seasonal variability of methane concentrations in ~~a~~this mountainous rural southern European region. The GIC3 station is located on the Spanish plateau, an area mainly characterized by livestock activity and where ~~the~~ transhumance is still practiced (Ruiz Perez and Valero Sáez, 1990). This is an ancestral activity consisting of the seasonal movement of ~~the livestock~~ livestock over ~~large~~ long distances to reach warmer regions during the winter ~~and~~together with a return to the mountains in summer where pastures are greener and more suitable for grazing activities (Ruiz Perez and Valero Sáez, 1990; López Sáez et al., 2009). ~~Particularly, the~~The livestock ~~lives~~leaves the GIC3 region to go to southern Spanish regions~~, such as Extremadura,~~ during the cold period. The enteric fermentation due to digestive processes in animals could thus be a significant CH_4 source in this area. The Unión de Pequeños Agricultores (UPA, 2009) reports that between 2004 and 2009 an average of 800,000 transhumant animals were hosted in Spain and 40,000 (5% of total) were counted in the province of Ávila (extension: 8,048 km^2), where the GIC3 station is located. According to the available literature, in this area 85% of livestock still performs transhumance, with 500 stockbreeders moving every winter from the Gredos Natural Park (GNP) to warmer areas of Spain, such as Extremadura (Ruiz Perez and Valero Sáez, 1990; López Sáez et al., 2009; Libro Blanco, 2013). Generally, this mobility of ~~the~~ cattle and ~~its~~ associated CH_4 emissions (i.e. a major regional CH_4 source) cannot easily be included in country-wide (annual) ~~bottom-up~~ inventories because it ~~is~~has not yet been properly quantified and reported by nations. The present study ~~wants~~aims to highlight the utility of ^{222}Rn as a tracer to retrieve independent GHGs fluxes on a monthly basis using atmospheric ^{222}Rn and CH_4 ~~concentrations~~ data. This work represents a first step ~~toward~~towards a better ~~further~~ characterization of ~~"mobile"~~transient sources, such as transhumant livestock for CH_4, which could help to improve national emissions inventories. Finally, it offers new CH_4 data for an under-sampled area which will help in the improvement of the regional and global methane budgets.

Formatted: Font: 10 pt, English (U.K.)

GIC3 is a new atmospheric station ~~thus~~so its location, the surrounding region and the instrumentation used at this station ~~have been~~are described in the methodology section of this manuscript. In the first part of the results section both the daily and seasonal changes in CH_4 ~~concentrations~~mixing ratios observed at the GIC3 station have been analysed in relation to ^{222}Rn and PBLH variability. In the second part, the ~~local~~nocturnal CH_4 fluxes and their monthly variability have been estimated by the Radon Tracer Method

(RTM), following Vogel et al. (2012), and using an emission inventory for CH_4 (EDGARv4.2). Both ~~source~~flux estimation methods have been applied ~~taking into account~~using the same source region as modelled by the atmospheric transport model ~~FLEXPARTv6~~FLEXPARTv9.0.2. The possible influence of ~~big~~large cities surrounding GIC3 and of seasonally changing meteorological conditions on the retrieved CH_4 fluxes has also been investigated. Finally, the difference in CH_4 fluxes between the ~~warm~~Cattle season, ~~defined by the presence of the~~when livestock is present in the GIC3 region, and the ~~cold~~No-Cattle season, when the transhumant cattle ~~migrates~~have migrated to the south of Spain, calculated using the RTM, has been estimated.

2 Methods

2.1 Study site: Gredos and Iruelas station (GIC3)

Formatted: Font: 10 pt, English (U.K.)

The Gredos and Iruelas station (GIC3) is located in a rural region of the Spanish central plateau (40.35ºN; 5.17ºE; 1440 m above sea level (a.s.l~~.),~~.)), as shown in Figure ~~1).~~S1 of the supplement. GIC3 is ~~set in~~located on the west side of the Gredos ~~Natural~~National Park (GNP), which has a total extension of 86,397 ha. The mountains of the GNP form the highest mountain range in the E-W orientated central mountain system~~ that divides the Iberian Peninsula in two parts.~~. The GNP ~~is located in~~has a, predominantly, granitic basement~~; this type of~~ and is thus covered by soil ~~presents~~with high activity levels of ^{228}U (Nazaroff and Nero, 1988). The average ^{222}Rn flux in this area is ~~of~~ about 70-100 Bq m^{-2} h^{-1} (e.g. López-Coto et al., 2013; Karstens et al., 2015~~)~~), which is almost twice the average radon flux in central Europe (Szegvary et al., 2009, López-Coto et al., 2013; Grossi et al., 2016). The vegetation ~~at~~in the GIC3 area is stratified according to ~~the~~ altitude and the main land use practice is a mixture of agro-forestry exploitation (~~Figure 1).~~EEA, 2013).

Formatted: Internet Link, Font: 12 pt

Formatted: Font: 10 pt, English (U.K.)

Formatted: Footer, Right

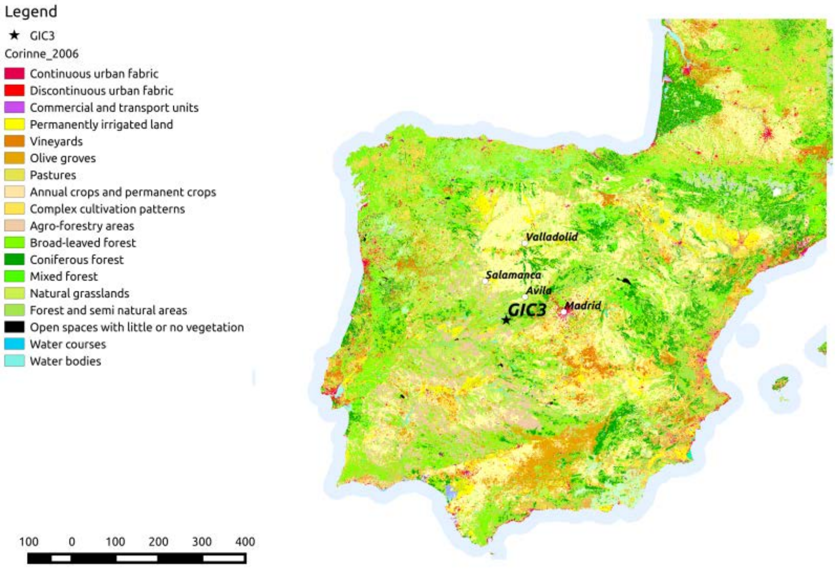

~~Figure 1. CORINE land cover map 2006 for Spain with GIC3 (star label) and surrounding large cities (Madrid, Salamanca, Valladolid and Avila).~~

~~Particularly, livestock~~Livestock farming is one of the main economic activities in the area around the GIC3 station (Ruiz Perez and Valero Sáez, 1990; López Saéz et al., 2009; MMA, 2016; Hernández, 2016). ~~The enteric fermentation due to digestive processes in animals can, thus, be a significant CH_4 source in this area. The Unión de Pequeños Agricultores (UPA, 2009) reports that between 2004 and 2009 an average of 800,000 transhumant animals were hosted in Spain and 40,000 (5% of total) were counted in the province of Ávila, where GIC3 station is located. According to the available literature, in this area 85% of livestock still performs transhumance, with 500 stockbreeders moving every winter from the GNP~~In the GNP the seasonal migration of livestock starts between November and December~~ to warmer areas of Spain, such as Extremadura (Ruiz Perez and Valero Sáez, 1990; López Sáez et al., 2009; Libro Blanco, 2013). In the GNP the seasonal migration of livestock starts in early November~~, when they travel to the south of the Iberian Peninsula, and they do not return until late May-mid June (Ruiz Perez and Valero Sáez, 1990). In Figure ~~S1~~S2 of the supplement, a map of the main Spanish transhumant paths is presented. ~~The path used by the livestock present at GIC3 region is presented as a zoom in subplot, indicating the entrance location (Puerto del Pico).~~ Unfortunately, no specific reports ~~with data about the mobility rate~~ of cattle ~~or a local livestock count for individual months of the year~~ mobility data are ~~not~~so far available for the GIC3 area.

Besides livestock activities, there are three small-sized to medium-sized water reservoirs and four medium-~~size~~sized to large cities in the wider area surrounding GIC3. ~~Several~~The water reservoirs as well as several activities present in ~~these~~the cities, e.g. landfills or waste water treatment plants, represent CH_4 sources which could also influence methane concentrations observed at the GIC3 station under specific

Formatted: Internet Link, Font: 12 pt

Formatted: Font: 10 pt, English (U.K.)

synoptic conditions. The water reservoirs are located in the west and north-west area of GIC3: i) The Gabriel and Galan reservoir with an extension of 4683 ha (40.25º N; -6.13º E; 80 km away from GIC3); (ii) Santa Teresa with an extension of 2663 ha (40.60º N; -5.58º E; 42 km away from GIC3); (iii) Almendra with an extension of 7940 ha (41.25º N; -6.26º E; 120 km away from GIC3). The metropolitan area of Madrid, which comprises about 6.3 million inhabitants, is situated ~~ca.~~approximately 120 km to the east of GIC3. Valladolid, located 150 km to the west of GIC3, is reported to have ~~ca.~~approximately 416~~.~~,000 inhabitants, while smaller cities like Salamanca (84 km to the north-west) and Ávila (55 km to the north-east) only have 229,000 and 59,000 inhabitants, respectively. More information about these four cities is reported in Table S1 of the supplement.~~.~~

Formatted: Font: 10 pt, English (U.K.)

Formatted: English (U.S.)

2.2 Atmospheric measurements of CH_4 and ^{222}Rn

2.2.1 Air sampling

Atmospheric CH_4, CO_2 and ^{222}Rn concentrations ~~are~~have been continuously measured since November 2012 at the GIC3 station (air inlet ~~at~~ 20 m above ground level (a.g.l.) tower). CH_4 and CO_2 are measured with a frequency of 0.2 Hz using a G2301 analyzer (Picarro Inc., USA~~; Crosson, 2008) with a frequency of 0.2 Hz.~~). Hourly atmospheric ^{222}Rn concentrations are measured using an Atmospheric Radon MONitor (ARMON) (Grossi et al., 2012; Grossi et al., 2016). A schematic diagram of the measurement set-up used at the GIC3 station is shown in Figure S3 of the supplement.

The Picarro Inc. G2301 analyzer is calibrated every two weeks using 4 secondary working gas standards, which are calibrated at the beginning and ~~at the~~ end of their lifetime against seven standards of the National Oceanic and Atmospheric Administration (NOAA) (calibration scales are WMO-CO_2-X2007 and WMO-CH_4-X2004 for CO_2 and CH_4, respectively). A target gas is analyzed daily for 20 minutes in order to check the stability and quality of the instrument~~. The~~ calibration. For the length of the study, the instrument ~~accuracy~~repeatability for CH_4 ~~is of~~was 0.80 nmol mol^{-1}, the long term reproducibility was 0.36 ~~ppb,~~nmol mol^{-1} and the observe bias was 0.81 nmol mol^{-1}. Previous values were calculated according to the definitions of the World Meteorological Organization (WMO~~).~~, 2009). The ARMON instrument was installed at the GIC3 station in collaboration with the Institute of Energetic Techniques of the Universitat Politècnica de Catalunya (INTE-UPC). The ARMON is a self-designed instrument based on α spectrometry of ~~-~~^{218}Po, collected electrostatically on a ~~passivated~~passive implanted detector. The monitor has a minimum detectable activity of ~~about~~ 150 mBq m^{-3} (Grossi et al., 2012). The performance of the ARMON ~~has been~~was previously tested against a widely used ^{222}Rn progeny monitor and good results ~~have been~~were observed (Grossi et al., 2016).

The responses of both the ARMON and ~~Picarro Inc.~~ G2301 analyzers are influenced by the air sample humidity level. Water correction factors for both instruments are empirically determined and corrected following Grossi et al. (2012) and Rella (2010~~) methodologies,~~), respectively.

Formatted: Footer, Right

2.2.2 ~~Drying~~Sample air drying system

Formatted: Font: Bold

The instruments used at the GIC3 station require a total flow of ~~3~~2.5 L min^{-1} of sample air dried to a water concentration lower than 1000 ppm to perform simultaneous measurements of GHGs and ^{222}Rn concentrations.

In the GIC3 inlet system, as shown in Figure S3 of the supplement, the sample air is passed through a Nafion® membrane (Permapure, PD-100T-24MPS) that exchanges water molecules with a dry counter-current air flow. The counter-current air flow is dried in a two~~-steps~~-step process, first through a cooling coil in a refrigerator at 3 ºC and a pressure of 5.5 barg, and then ~~using~~ a cryotrap is used at -70 ºC ~~at~~and a pressure of 1.5 barg. Multiple cryotraps are selected with electrovalves in order to increase the autonomy of the system to about 2 months. The typical water content of sample air inside the instruments is between 100 and 200 ppm.

Formatted: Left

2.2.3 Meteorological observations

Meteorological variables are continuously measured at the GIC3 tower. The canopy around the tower is below 20 ~~cm and the~~m. The area surrounding ~~area~~ the GIC3 station is ~~quite~~ hilly as shown on the topographic map of Figure S1 of the supplement. The tower is equipped with: (1) Two-dimensional sonic anemometer (WindSonic, Gill Instruments) for wind speed and direction (accuracies of ± 2 % and ± 3 º, respectively); (2) Humidity and temperature probe (HMP 110, Vaisala) with an accuracy of ± 1.7 % and ± 0.2 ºC, respectively; (3) Barometric pressure sensor (61302V, Young Company) with an accuracy of 0.~~2h Pa~~2 hPa (at 25 °C)~~-~~ and 0.3 hPa (from -40 to +60 °C). All the accuracies refer to the manufacturer's specifications.

Formatted: Font: 10 pt, English (U.K.)

2.3 Planetary boundary layer height (PBLH)

Formatted: Font: 10 pt, Bold, English (U.K.)

Planetary boundary layer height (PBLH) data used in this analysis have been extracted from the operational high resolution atmospheric model of the European ~~Center~~Centre for Medium-Range Weather Forecasting (ECMWF-HRES) (ECMWF, 2006) for the period of interest (January 2013 - December 2015) ~~at~~for the GIC3 area. This model stores output variables every 12 hours (at 00.00 UTC and 12.00 UTC) with a temporal resolution output of 1 h and with forecasts from +00h to +11h. The horizontal spatial resolution of the model is about 16 km. In the ECMWF-HRES model the calculation of the PBLH is based on the bulk Richardson number (Ri) (Troen and Mahrt, 1986). ~~Seidel et al. (2012) underlined that several factors contribute to uncertainties in these calculations, including the critical R~~$_{i}$ ~~value used for the calculation.~~ As regards the reliability of modelled PBLH data, Seidel et al., (2012) have shown that data limitations in vertical profiles introduce height uncertainties that can exceed 50% for shallow boundary layers (<1 km), but are generally <20% for deeper boundary layers. In addition, they compared

Formatted: Not Superscript/ Subscript radiosonde observations with re-analysis and climate models and showed that these latter two produce deeper layers due to the difficulty in simulating stable conditions.

2.4 CH_4 fluxes

2.4.1 ~~2.4.1 FLEXPART_RTM~~ CH_4 fluxes based on FLEXPART footprints and the Radon Tracer Method

The RTM is a well-known method (e.g. Hammer and Levin 2009) and it has been used in this study, following ~~the implementation described in~~ Vogel et al. (2012) in order to obtain observation-based estimates of ~~the~~ nocturnal CH_4 fluxes at GIC3. The RTM uses atmospheric measurements of ^{222}Rn and measured, or modelled, values of ~~its~~ ^{222}Rn fluxes together with atmospheric ~~concentrations~~mixing ratios of ~~an~~a gas of interest ~~gas~~, i.e. CH_4, in order to retrieve the net fluxes of this gas (e.g. Hammer and Levin 2009; Grossi et al., 2014).

This method is based on the ~~main~~ assumption that the nocturnal lower atmospheric boundary layer can be described as a well-mixed box of air (Schmidt et al. 1996; Levin et al., 2011; Vogel et al., 2012). ~~In this atmospheric box the variation of the concentration of any tracer with time $C_i(t)$ will be proportional to the flux of the tracer $F_i(t)$ and inversely proportional to the height of the boundary layer ($h_i(t)$) (Eq.1; e.g. Griffiths et al., 2012; Grossi et al., 2014).~~

~~(1)~~

The boundary layer is considered homogeneous within the box and with a time varying height. No significant horizontal advection is considered due to stable atmospheric conditions (Griffiths et al., 2012). In this atmospheric volume the variation of the concentration of any tracer (shown with the subindex *i*) with time $C_i(t)$ will be proportional to the flux of the tracer $F_i(t)$ and inversely proportional to the height of the boundary layer $h(t)$ (Eq.1; e.g. Galmarini, 2006; Griffiths et al., 2012; Vogel et al., 2012; Grossi et al., 2014).

$$\frac{dC_i(t)}{dt} \propto F_i(t) \cdot \frac{1}{h(t)} \qquad (1)$$

Applying Eq. 1 for both ^{222}Rn and CH_4, Eq. 2 is obtained, with a dimensionless conversion factor c derived from the observed slope of the concurrent concentration increase of both gases:

Formatted: Font: Bold

Formatted: Font: 10 pt, Bold, English (U.K.)

Formatted: Font: 10 pt, English (U.K.)

Formatted: Outline numbered + Level: 3 + Numbering Style: 1, 2, 3, … + Start at: 1 + Alignment: Left + Aligned at: 0 cm + Tab after: 0 cm + Indent at: 1.27 cm

Formatted: Font: 10 pt, English (U.K.)

Formatted: English (U.S.)

Formatted: English (U.S.)

Formatted: English (U.S.)

Formatted: English (U.S.)

Formatted: Not Highlight

Formatted: English (U.S.)

Formatted: Footer, Right

$$\frac{\frac{dC_{CH_4}(t)}{dt}}{\frac{dC_{^{222}Rn}(t)}{dt}} \cdot F_{^{222}Rn} = c \cdot F_{^{222}Rn} = FR\_CH_4 \quad (2).$$

Observing the concentration increase of two gases that fulfil the above assumptions, here CH_4 and ^{222}Rn~~,~~ ~~and knowing~~. If the flux of ^{222}Rn is known, then the flux of CH_4 can be calculated (Levin et al., 2011). A description of the specific criteria used to implement the RTM~~, which include selection criteria to reject situations with unstable atmospheric conditions, remote influences on the concentration and outliers detection,~~ can be found in detail in Vogel et al. (2012). Grossi et al. (2014) previously applied the RTM for the first time at the GIC3 station using only a 3-~~months~~month dataset and with a constant (in time and space) ^{222}Rn flux~~.~~ of 60 Bq m^{-2} h^{-1}. Here, in order to apply the RTM to retrieve a time series of CH_4 fluxes (~~FLEXPART_RTM~~FR_CH_4) during 2013-2015 at the GIC3 station and to compare these results with ~~the ones~~those obtained using a bottom-up inventory for methane (~~FLEXPART_EDGAR~~FE_CH_4), we used the following extensive ~~setup~~set-up:

1. A nocturnal window between 20.00 UTC and 05.00 UTC was selected for ~~the~~each single night analysis in order to utilize only accumulation events when atmospheric concentrations of both CH_4 and ^{222}Rn had a positive concentration gradient due to positive net fluxes under stable boundary layer conditions;
2. A data selection criterion based on a threshold of $R^2 \geq 0.8$ for the linear correlation between ^{222}Rn and CH_4 was used to reject events with low linear correlation between the atmospheric concentrations of both gases;
3. An *effective* ~~local~~ radon flux influencing the GIC3 station each night from 2013 to 2015 was calculated by coupling local radon flux data, obtained using the ~~UHU model~~output for the local pixel containing the GIC3 station of the model ~~(~~developed by López-Coto et al~~.,~~. (2013), with the footprints calculated by ECMWF-FLEXPART model (version ~~6~~9.02) (Stohl, 1998). ~~Radon~~Local radon flux data were calculated as explained in the following paragraph ~~and~~, while the footprints obtained are described in ~~section~~Section 2.4.3.

The radon flux model ~~(~~of Huelva University (from now on named the UHU model) employed in this work has been described in detail by López-Coto et al. (2013). By using this model, a time-dependent inventory was calculated for the period 2011–2014 by employing several dynamic inputs, namely soil moisture, soil temperature~~,~~ and snow cover thickness. These data were obtained directly from Weather Research and Forecasting (WRF) simulations (Skamarock et al., 2008). A domain of 97 x 97 grid cells ~~centered in~~centred on Spain with a spatial resolution ~~for grid of 0.2 degrees~~ of 27 x 27 km^2 and a temporal resolution of 1 hour~~,~~ was defined ~~(López-Coto et al., 2013).~~. ^{222}Rn flux data calculated using this model were only available until November 2014 due to a lack of WRF simulations. In order to ~~fulfil the~~obtain data for this period when modelled ^{222}Rn flux data were not available, from December 2014 to December 2015, a seasonal and monthly climatology was calculated by using the UHU data set ~~of UHU~~ model for the years 2011-2014. Karstens et al. (2015) compared the ^{222}Rn flux values calculated over Europe by

Formatted: Subscript
Formatted: Font: 10 pt, English (U.K.)
Formatted: Font: 10 pt, English (U.K.)
Formatted: Font: 10 pt, English (U.S.)
Formatted: Font: 10 pt, English (U.K.)
Formatted: Font color: Custom Color(RGB(34,34,34))
Formatted: Font color: Custom Color(RGB(34,34,34))
Formatted: Font color: Custom Color(RGB(34,34,34))
Formatted: Font color: Custom Color(RGB(34,34,34))
Formatted: Font color: Custom Color(RGB(34,34,34))
Formatted: Font color: Custom Color(RGB(34,34,34))
Formatted: Font color: Custom Color(RGB(34,34,34))
Formatted: Font color: Custom Color(RGB(34,34,34))
Formatted: Font color: Custom Color(RGB(34,34,34))
Formatted: Font color: Custom Color(RGB(34,34,34))
Formatted: Font color: Custom Color(RGB(34,34,34))
Formatted: Font color: Custom Color(RGB(34,34,34))
Formatted: Font color: Custom Color(RGB(34,34,34))
Formatted: Font color: Custom Color(RGB(34,34,34))

their model to UHU values and to long-term direct measurements of ^{222}Rn exhalation rates in different areas of Europe. They found a generally 40% higher ^{222}Rn exhalation rate on their map than estimated by the UHU map over Europe. This previous result has been taken into consideration within the present study to better interpret the obtained data.

~~**2.4.2 FLEXPART_EDGAR_CH_4 fluxes**~~

2.4.2 CH_4 fluxes based on FLEXPART footprints and the EDGARv4.2 inventory grid map

Bottom-up CH_4 fluxes influencing the GIC3 station were estimated by using the footprints calculated by the ECMWF-FLEXPART model (obtained as described in ~~section~~Section 2.4.3) and the Emissions Database for Global Atmospheric Research (EDGAR) version 4.2 (EDGAR, 2010). The EDGAR inventory, developed by the European Commission- Joint Research Centre- and the Netherlands Environmental Assessment Agency, includes global anthropogenic emissions of GHGs and air pollutants by country ~~and~~ on a spatial grid. The EDGAR version used in the present study provides ~~spatial (cells of 0.1 degree)~~global annual ~~mean~~ CH_4 emissions ~~globally~~on a 0.1 degree (11 km) resolution for the year 2010. All major anthropogenic source sectors, e.g. waste treatment, industrial and agricultural sources (e.g. enteric fermentation) are included, whereas natural sources (e.g. wetlands or rivers) are not. The spatial allocation of emissions on 0.1 degree by 0.1 degree grid cells in EDGAR has been built up by using spatial proxy datasets with the location of energy and manufacturing facilities, road networks, shipping routes, human and animal population density and agricultural land use. UNFCCC reported national sector totals are then removed with the given percentages of the spatial proxies over the country's area (EDGAR, 2010). Figure 1 shows the EDGAR inventory grid map extracted for Spain.

The influence of the emissions associated ~~to~~with the cities surrounding the region of GIC3 was also modelled using this inventory to better understand their impact. In Table S1 of the supplement the coordinates of the upper and lower corners of the areas used to describe the location of the metropolitan areas over the EDGAR inventory are reported.

Formatted: Font: 10 pt, English (U.K.)
Formatted: Font: Not Bold
Formatted: Font color: Custom Color(RGB(34,34,34))
Formatted: Font color: Custom Color(RGB(34,34,34))
Formatted: Font color: Custom Color(RGB(34,34,34))
Formatted: Font color: Custom Color(RGB(34,34,34))
Formatted: Font color: Custom Color(RGB(34,34,34))
Formatted: Font color: Custom Color(RGB(34,34,34))
Formatted: Internet Link, Font: 12 pt, Font color: Custom Color(RGB(34,34,34)), Spanish (International Sort), Pattern: Clear (White)
Formatted: Font color: Custom Color(RGB(34,34,34))
Formatted: Internet Link, Font: 12 pt, Font color: Custom Color(RGB(34,34,34)), Spanish (International Sort), Pattern: Clear (White)
Formatted: Font color: Custom Color(RGB(34,34,34))
Formatted: Font color: Custom Color(RGB(34,34,34))
Formatted: Font color: Custom Color(RGB(34,34,34))
Formatted: Font color: Custom Color(RGB(34,34,34))
Formatted: Font color: Custom Color(RGB(34,34,34))
Formatted: Font: 10 pt, English (U.K.)
Formatted: Line spacing: single
Formatted: Font: 10 pt, English (U.K.)
Formatted: Footer, Right

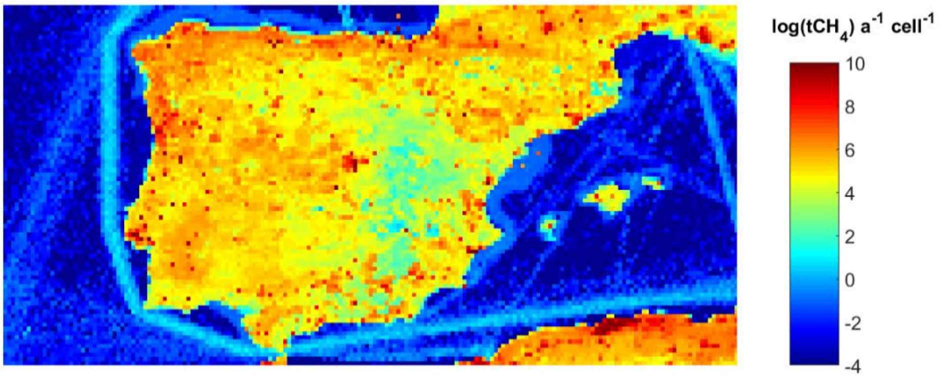

Figure 1. CH_4 EDGARv4.2 inventory grid map extracted for Spain (year 2010).

2.4.3 Footprints

The ~~lagrangian~~Lagrangian particle dispersion model ~~FLEXPARTv6~~FLEXPARTv9.0.2 has been extensively validated and is nowadays widely used by the scientific community to calculate atmospheric source-receptor relationships for atmospheric gases and organic particles (e.g. Stohl, 1998; ~~Sthol~~Stohl et al., 2005; Arnold et al., 2010; Font et al., 2013; Tohjima et al., 2014). FLEXPART allows ~~the~~ computation of the trajectories of virtual air parcels arriving at the receptor point, i.e. the GIC3 station, at a specific time. FLEXPART has been applied here to calculate 24 h backward trajectories of 10,000 virtual air parcels starting at 00.00 UTC for each night of the period 2013-2015. Each back trajectory simulation was run with a time-step output of 3 h. Meteorological data from the operational ECMWF-HRES model with a resolution of 0.2 degrees were used as input fields for the FLEXPART modelling. The FLEXPART output domain resolution was ~~of~~ 0.2 degrees. The domain was set at (25ºN, 40ºW) for the lowest left corner and (65ºN, 10ºW) for the upper right corner. A nested output domain of 0.05 degrees resolution was defined at (37ºN, 12ºW) for the lowest left corner and (43ºN, 0ºE) for the upper right corner. The FLEXPART model accounts for both the vertical and horizontal position of the virtual air parcels and their residence time in each grid cell. This information allows ~~estimating~~ the influence of ~~the~~ atmosphere-surface exchange to be estimated on the observed concentrations if air parcels are within the boundary layer. A maximum height of 300 m a.g.l. has been selected for the footprint analysis following Font et al. (2013).

The average nocturnal footprint for the period 2013-2015 is presented in Figure 2. The footprints obtained for the nested FLEXPART domain were combined with the EDGAR inventory map for CH_4 emissions (EDGAR, 2010) and with the UHU ^{222}Rn flux inventory map (López-Coto et al., 2013), separately, in order to obtain the time series of modelled CH_4 and *effective* ^{222}Rn fluxes. The resulting mean flux ~~F_c~~F_i(S,~~T~~t_n), for each gas ~~C~~$_i$, at the receptor S (GIC3 station) and ~~at time T~~for each night t_n, with n ranging over the 3-year period, is thus given by Eq. ~~2:~~3:

Formatted: Font: 10 pt, English (U.K.)

Formatted: Font: 10 pt, German (Germany)

~~(2)~~

~~where Fc~~ $F_i(S,t_n) = \sum_{t=t_{no}}^{t=t_n} \sum_x F_i(x,t_n) * w(x,T)$ (3)

where t ranges between the 24h of back-trajectories, F_i(x,t) denotes the flux of a given grid cell x at time t derived from the EDGAR or UHU inventory map, separately. The weighting factor of each grid cell w(x,~~t~~T) is calculated using the FLEXPART footprint for each night t_n over the 3~~ years~~ year period and it has been calculated by normalizing the residence time of each grid cell over the nested domain~~,~~ and during the 24 h back-trajectories (T), as given by Eq. 4:

Formatted: Font: 10 pt, English (U.K.)

$$\sum_{x,t}^{T} w(x,t) = 1 \quad (4)$$

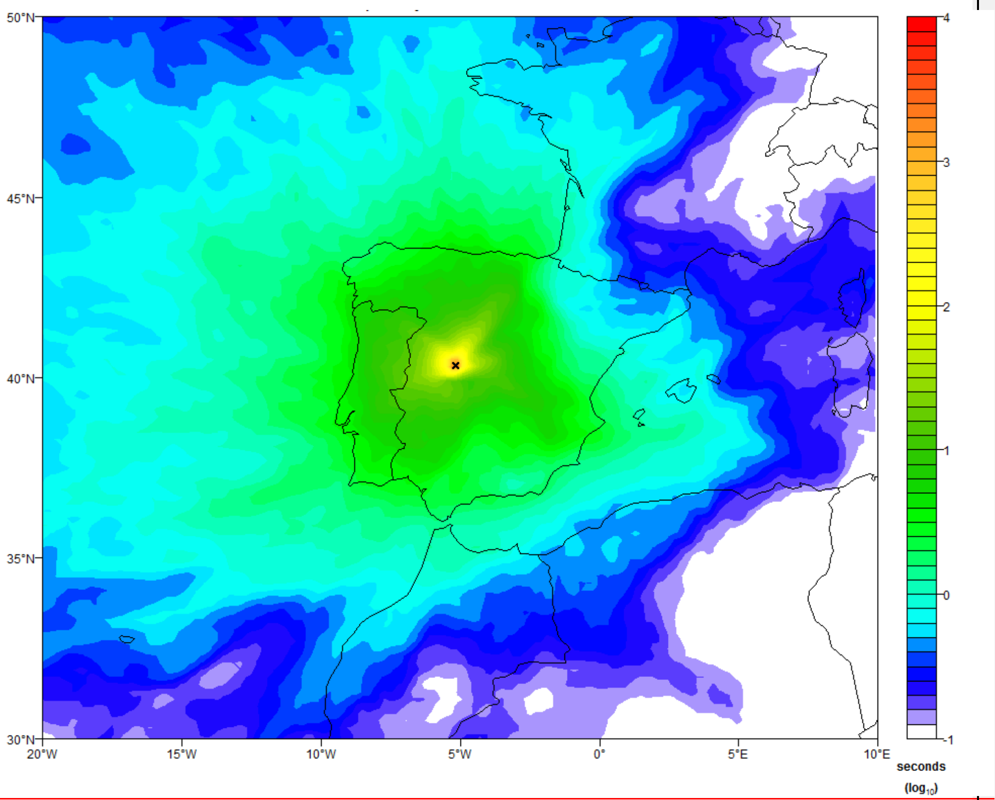

Figure 2. Average nocturnal FLEXPART footprint for the 2013-2015 period (residence time t is on the logarithmic scale).

Formatted: Footer, Right

3 Results

In ~~the present~~this section we present the results of the daily and seasonal atmospheric CH_4 variability at GIC3 station analysed using a record of 3-~~years~~year hourly CH_4 and ^{222}Rn time series. Unfortunately, due to problems in the air sample system~~ the~~, data for 11 % of the ~~total data set was~~time period are not available, mainly in the summer of 2013.

~~Since~~ Grossi et al. (2016) presented a complete characterization of the main meteorological conditions and ^{222}Rn behaviour at ~~GIC3, along with other Spanish~~the ClimaDat stations~~,~~, including GIC3, and we will use these previous results to interpret ~~the variability of the~~ atmospheric processes and the variability of CH_4 ~~concentrations~~mixing ratio, as well as to ~~interpret~~understand the dominating wind regimes for CH_4 flux data analysis (~~Figures S2 and S3~~Figure S4 of the supplement ~~present the daily and monthly ^{222}Rn variations and~~presents the monthly wind regimes observed at the GIC3 station both for daytime and night-time).

3.1. Statistics of the daily and seasonal atmospheric CH_4 variability

The 3-~~years~~year hourly time series of atmospheric CH_4 ~~concentrations~~mixing ratios measured at ~~the rural area of~~ GIC3 shows a ~~mean value and a standard error of 1914.3 ± 0.3 ppb, with an inter quartile range of 1887-1930 ppb. The median value over the dataset is~~ median value of 1904.5 ~~ppb~~nmol mol^{-1} with an absolute deviation of 29.6 ~~ppb~~nmol mol^{-1}. The boxplots in Figure ~~2~~3 present the medians of the atmospheric CH_4 mixing ratios and ^{222}Rn concentrations measured at the GIC3 station over the dataset on an hourly (left ~~panel~~panels) and a monthly (right ~~panel~~panels) basis. Monthly means have been calculated separately for daytime (07.00 UTC – 18.00 UTC) and night-time (19.00 UTC – 06.00 UTC).

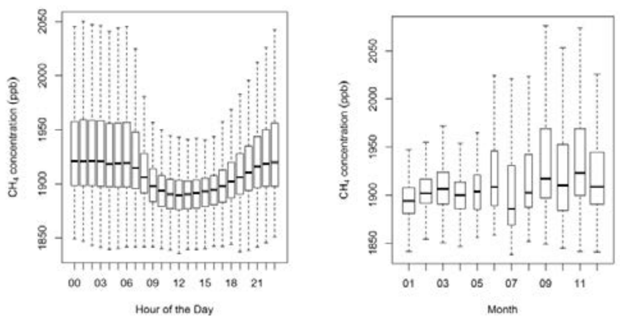

Formatted: Font: 10 pt, English (U.K.), Pattern: Clear (Red)

Formatted: Pattern: Clear (Red), Not Highlight

Formatted: Font: 10 pt, English (U.K.)

Formatted: English (U.S.)

Formatted: Pattern: Clear (Yellow)

Formatted: Pattern: Clear (Yellow), Not Highlight

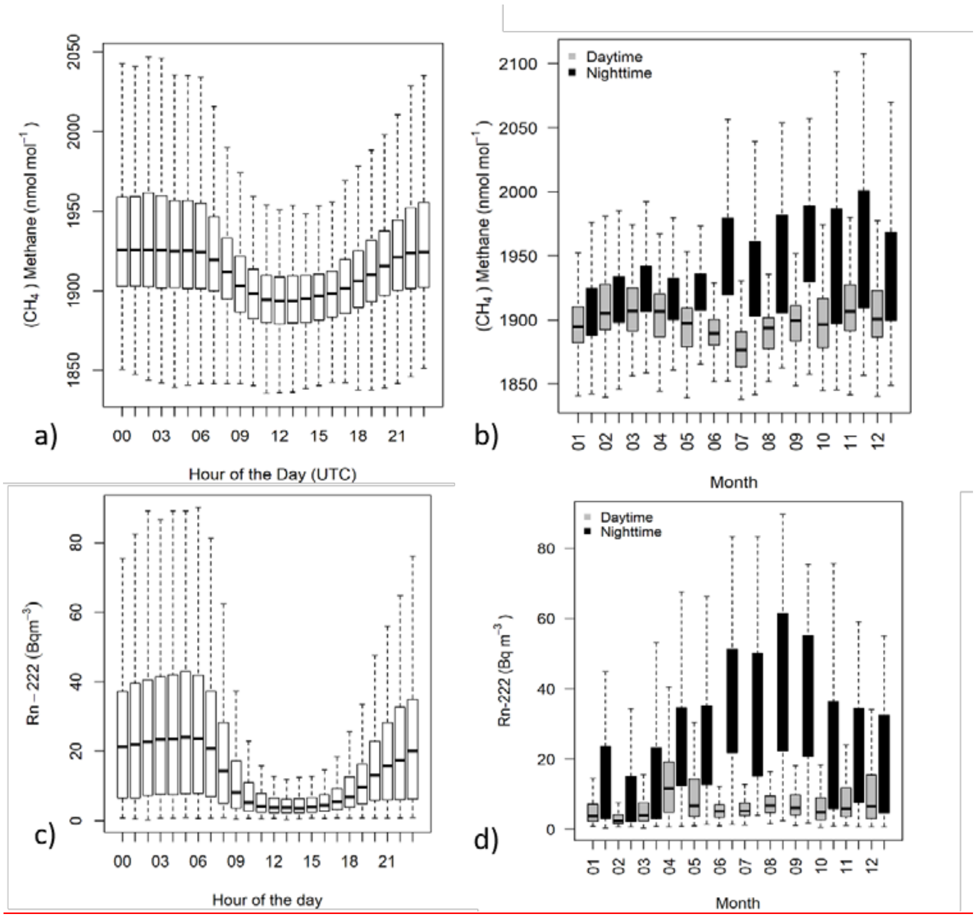

Figure ~~2~~3. Boxplots of hourly (~~left panel~~a,c) and monthly (~~right panel~~b,d) atmospheric CH_4 mixing ratios (a,b) and ^{222}Rn concentrations (c,d) measured from January 2013 to December 2015 at the GIC3 station. For each median (black bold line) the 25th (Q1; lower box limit) and 75th (Q3; upper box limit) percentiles are reported in the plot. The lower whisker goes from Q1 to the smallest non-outlier in the data set, and the upper whisker goes from Q3 to the largest non-outlier. Outliers are defined as >1.5 IQR or <1.5 IQR (IQR: Interquartile Range).

Formatted: Font: 10 pt, English (U.S.)

Formatted: Font: 10 pt, English (U.S.)

Formatted: Font: 10 pt, English (U.S.)

Formatted: Font: 10 pt, English (U.S.)

Formatted: Font: 10 pt, English (U.S.)

Formatted: Font: 10 pt, English (U.S.)

The maximum hourly median methane mixing ratio measured within the 3-year observation period is 1921.1 nmol mol^{-1} and is observed at 03.00 UTC, whereas the minimum hourly median value of 1889.9 nmol mol^{-1} is observed at 13.00 UTC. The absolute standard deviation of the hourly median is 16.97 nmol mol^{-1}. The hourly median daily amplitude at this station, between the minimum and the maximum, is 31.18 nmol mol^{-1}. CH_4 concentrations usually start decreasing at GIC3 in the morning at around 07.00 UTC and 08.00 UTC and begin to increase again in the afternoon at around 17.00 UTC and 18.00 UTC. Night-time CH_4 concentrations present an absolute standard deviation of 60 nmol mol^{-1}, while for daytime concentrations it is 30 nmol mol^{-1}. The same pattern is observed in the daily cycle of atmospheric ^{222}Rn (Grossi et al., 2016). Monthly daytime and night-time medians of CH_4 mixing ratios and ^{222}Rn

Formatted: Footer, Right

concentrations show different patterns, as seen in Figure 3 (B,d). The night-time monthly medians of methane mixing ratio measured in the months between June and December look higher than those measured between January and May. Night-time monthly medians of measured ^{222}Rn concentration are highest between July and August.

3.2 Daily and seasonal PBLH variability

Figure 4 shows the hourly median (a) and the monthly median (b) variability of the PBLH data extracted from the ECMWF-HRES model for the grid containing the GIC3 station. On a daily basis the hourly median of the PBLH reaches its minimum during night-time between 23.00 UTC and 07.00 UTC. The PBLH starts to increase at around 08.00 UTC, reaching its maximum between 14.00 UTC and 16.00 UTC and then decreases again after 17.00 UTC. On a monthly basis, the daytime monthly median PBLH reaches its minimum during the winter months of January and December, while it reaches its maximum in the summer months. The highest night-time monthly medians for the PBL heights are observed in winter. The daytime monthly PBLH medians present a quite symmetric distribution (around July as a centre-line), similar to the night-time monthly ^{222}Rn medians (Figure 3d).

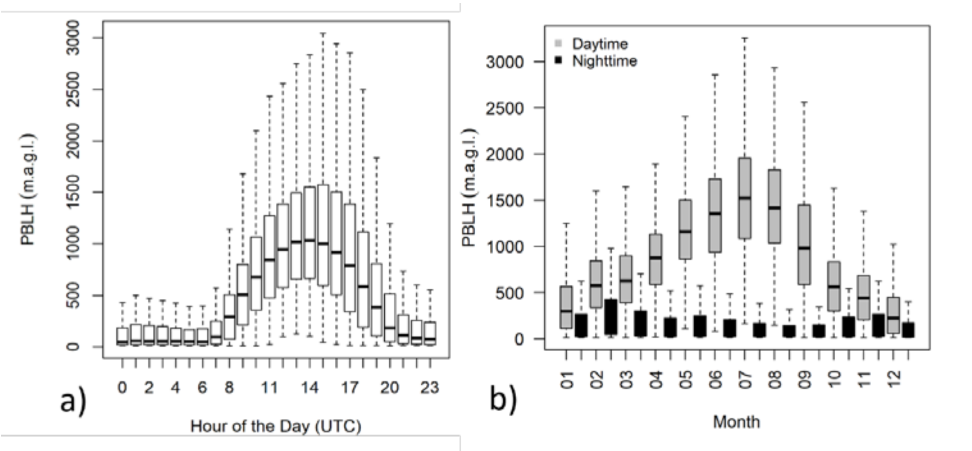

Figure 4 Boxplots of hourly (a) and monthly (b) PBLH data extracted from the ECMWF-HRES model for the period January 2013 - December 2015 at the GIC3 station. For each median (black bold line) the 25th (Q1; lower box limit) and 75th (Q3; upper box limit) percentiles are reported in the plot. The lower whisker goes from Q1 to the smallest non-outlier in the data set, and the upper whisker goes from Q3 to the largest non-outlier. Outliers are defined as >1.5 IQR or <1.5 IQR (IQR: Interquartile Range).

~~The maximum hourly median methane concentration measured within the 3 years of observations is 1921.1 ppb and is observed at 03.00 UTC, whereas the minimum median value of 1889.9 ppb is observed at 13.00 UTC. The absolute standard deviation of the median is 16.97 ppb. The median daily amplitude at~~

Formatted: Normal, Left, Line spacing: single, Tab stops: 1 cm, Left + 1.27 cm, Left

Formatted: Font: 10 pt

~~this station, between the minimum and the maximum, is of 31.18 ppb. CH_4 concentrations usually start decreasing at GIC3 in the morning around 07.00 UTC and 08.00 UTC and begin to increase again in the afternoon around 17.00 UTC and 18.00 UTC. Nighttime CH_4 concentrations present an absolute standard deviation of 60 ppb while for daytime concentrations it is of 30 ppb. For the monthly medians, Figure 2 (right panel) shows that atmospheric median methane concentrations range between 1885.8 ppb and 1923.1 ppb. Between June and November, excluding July, a general increase of methane concentrations is observed. Indeed, monthly median values range in these months is between 1908.6 ppb and 1923.1 ppb.~~

~~3.2 Daily and seasonal PBLH variability~~

~~Figure 3 shows the daily and seasonal variability of the PBLH at GIC3 station. It can be observed that on a daily basis the PBLH reaches its minimum between 01.00 UTC and 07.00 UTC. Indeed, within this interval median PBLH values present minima of 45 m a.g.l. The PBLH starts to increase around 08.00 UTC, reaching its maximum between 14.00 UTC and 16.00 UTC and then decreases again after 17.00 UTC. The maximum median PBLH value is 1037 m a.g.l. The absolute standard deviation is 283 m a.g.l.. On a monthly basis, the median PBLH reaches its minimum during winter months, January and December, with a value of 204 m a.g.l. The highest PBL heights are observed in summer months with typical values around 595 m a.g.l. and an absolute standard deviation of 204 m a.g.l.. It is noteworthy noting that the monthly PBLH is quite symmetric (around July as center line) and many months in fall and spring experience similar PBLH distributions.~~

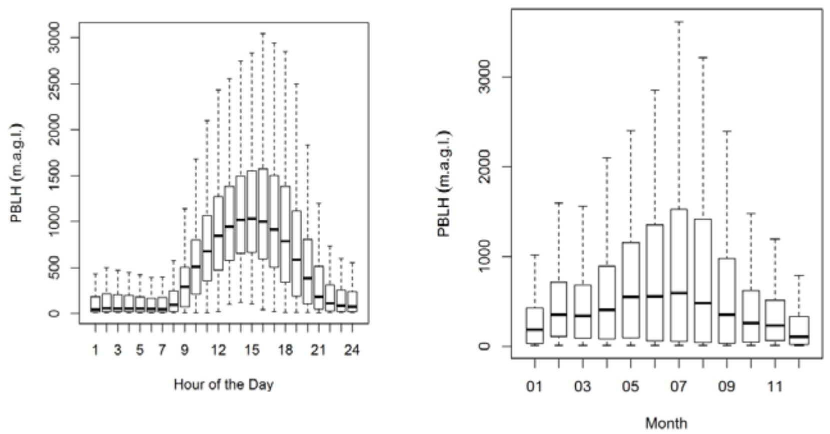

~~Figure 3 Boxplots of hourly (left panel) and monthly (right panel) PBLH data extracted from ECMWF-HRES model for the period January 2013 - December 2015 at GIC3 station. For each median (black bold line) the 25th (Q1; lower box limit) and 75th (Q3;~~

Formatted: Normal (Web), Justified, Line spacing: 1.5 lines, Tab stops: Not at 1 cm

Formatted: Footer, Right

~~upper box limit) percentiles are reported in the plot. The lower whisker goes from Q1 to the smallest non-outlier in the data set, and the upper whisker goes from Q3 to the largest non-outlier. Outliers are defined as >1.5 IQR or <1.5 IQR (IQR: Interquartile Range).~~

3.3 Comparison between CH_4 and ^{222}Rn variability

A comparison of the daily and seasonal variability of the atmospheric concentrations of ^{222}Rn and CH_4 in relation to ~~the~~ changes in ~~the~~ height of the PBL at the GIC3 station (2013-2015) is presented in Figures ~~4~~5 and ~~5~~6, respectively.

The daily evolution of hourly means of the ^{222}Rn atmospheric concentrations (Figure ~~4~~5, upper panel) implies that ~~during the daytime (8.00 UTC-17.00 UTC),~~on a daily time-scale, when ^{222}Rn flux can be considered fairly constant (e.g. ~~Lòpez~~López-Coto et al., 2013), PBLH variations drive the increase or decrease of the atmospheric ^{222}Rn concentrations. In this sense, ^{222}Rn seems to be an excellent predictor of PBLH (and vice~~-~~-versa) on a daily time-scale. Looking at the hourly means of the atmospheric CH_4 ~~concentrations~~mixing ratios (Figure ~~4~~5, lower panel~~)~~), we can observe that ~~the daily~~ methane ~~evolution also~~ decreases ~~in agreement with the increase of~~ as the PBLH increases, as ~~it~~ was observed for ^{222}Rn. However, ~~CH_4 data seem to show a hysteresis cycle. Between 16.00 UTC~~ between 12.00 UTC and 18.00 UTC higher values in CH_4 ~~concentrations~~mixing ratios relative to the values observed ~~during~~between 10.00 UTC and 12.00 UTC are observed, which have similar PBLH conditions~~.~~ and could indicate some daily variability in the methane fluxes.

Formatted: Spanish (International Sort)

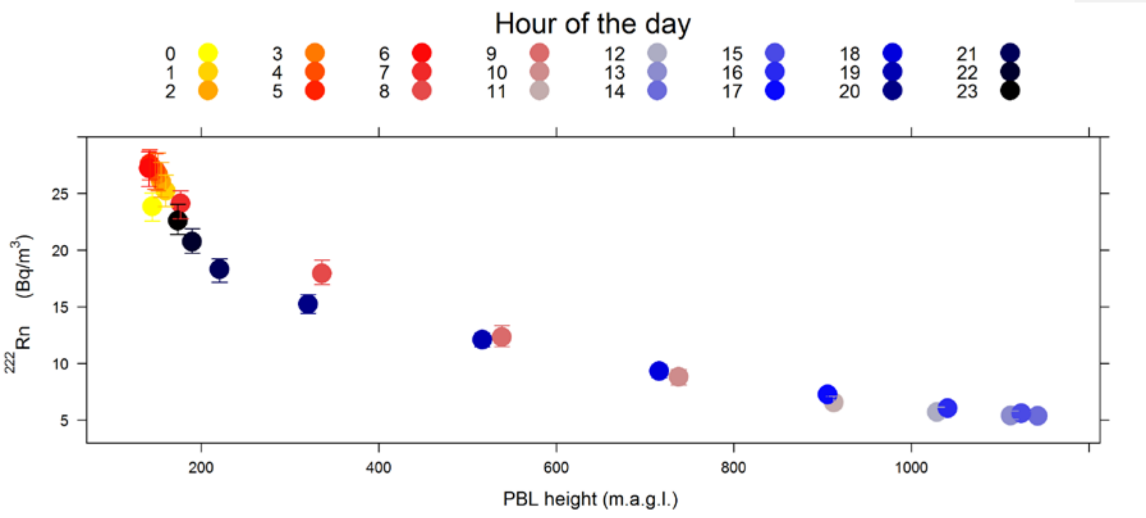

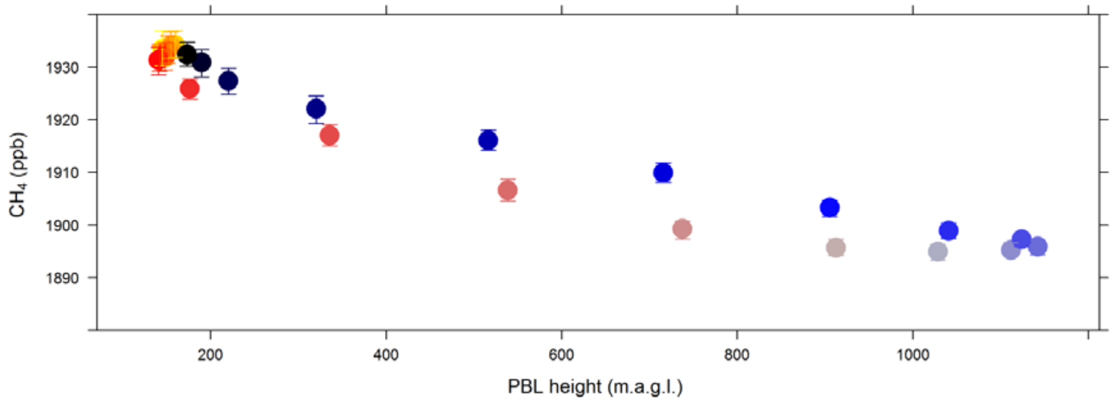

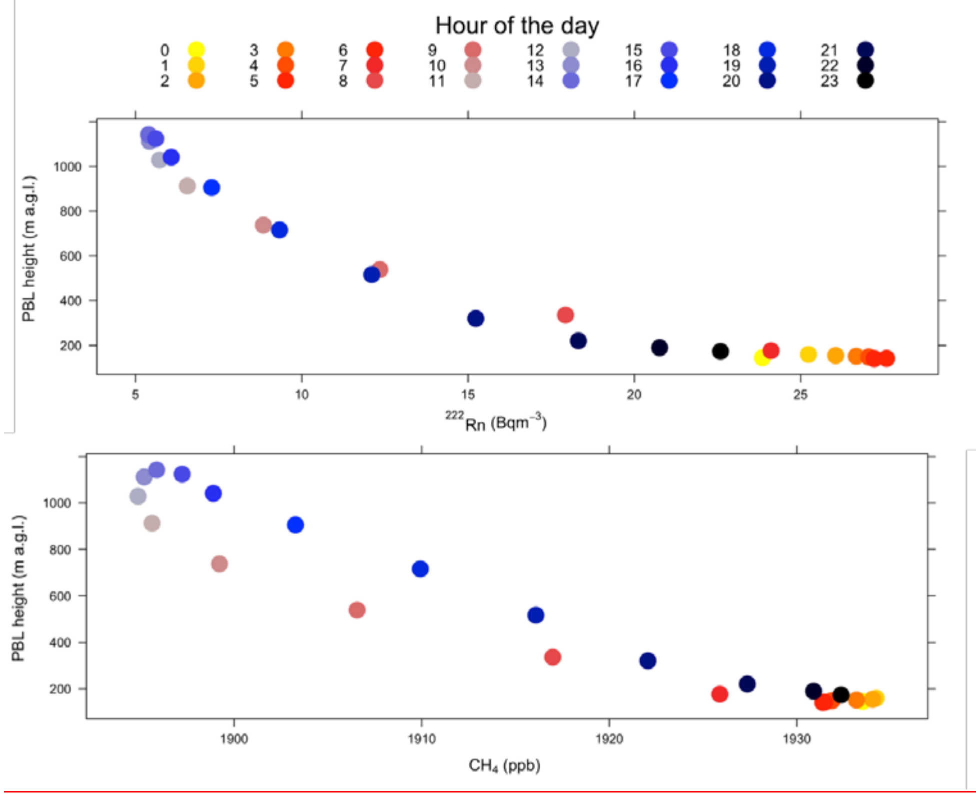

Figure ~~4~~5 Relation between hourly means of atmospheric CH_4 (lower panel) and ^{222}Rn (upper panel) concentrations measured during 2013-2015 at the GIC3 station and ECMWF data of PBLH ~~at~~for the same area and ~~during~~for the same time interval.

Formatted: English (U.S.)

To interpret the monthly variability, the daily amplitude for each gas, i.e. ~~$\Delta^{222}Rn_{daily}$~~Δ^{222}Rn for radon and ~~ΔCH_{4daily}~~ΔCH_4 for methane, was calculated in order to subtract the influence of the changing daily background contribution measured at the GIC3 station. ~~Then,~~ Δ^{222}Rn is defined as the difference between average ~~nighttime~~night-time concentration data (~~18~~19.00 UTC - ~~07~~06.00 UTC) versus average daytime

Formatted: Footer, Right

(~~08~~07.00 UTC-~~17~~18.00 UTC) ~~concentrations~~concentration data (Eq. ~~3~~5). ΔCH_4 has been calculated accordingly.

~~(3)~~

$$\Delta^{222}Rn = {}^{222}Rn_{nighttime} - {}^{222}Rn_{daytime} \quad (5)$$

Field Code Changed

Figure ~~5~~6 reveals that monthly amplitudes increase in summer, when the daytime PBLH ~~increase~~increases very strongly due to vertical mixing (see Figure ~~3~~4). This general tendency is found both for ^{222}Rn and CH_4 concentrations. ^{222}Rn concentrations amplitudes in autumn are higher than in ~~spring~~winter under the same PBLH conditions~~.~~ (Figure 6, upper panel). This could indicate that some process, other than PBLH, is driving this difference ~~of~~in the ^{222}Rn concentrations. ~~Looking at the~~In Figure ~~6, it can be observed~~7 we observe how ~~changes~~ the ~~seasonal~~monthly ^{222}Rn ~~fluxes~~flux calculated by the UHU model (presented in ~~section~~Section 2.4~~).~~) changes.

In agreement with ~~the results discussed by~~ Grossi et al. (2016), ~~the~~we find a lower ^{222}Rn flux at GIC3 ~~is lower~~ during winter~~,~~ due to snow cover events and low temperatures, which prevent ^{222}Rn diffusion from the soil. ~~Then, it~~The ^{222}Rn flux then increases almost two-fold and three-fold during the autumn and summer months, respectively. This is due to drier soil conditions and the high gradient of temperature in the surface atmospheric layer which facilitates ~~^{222}Rn to~~the escape of ^{222}Rn from the pores of the granitic soil (Nazaroff and Nero, 1988). This seasonality of the ^{222}Rn flux could be the main cause of the increased atmospheric $\Delta^{222}Rn$ under the same PBLH conditions.

Monthly variations of ΔCH_4 shown in Figure ~~5~~6 (bottom panel) ~~also~~ display no clear simple correlation with PBLH. ~~Indeed,~~ ΔCH_4 appears ~~independent from~~to be higher between the months of June and December irrespective of the corresponding PBLH values~~, displaying the lowest values between December and May and the highest values between June and November~~.

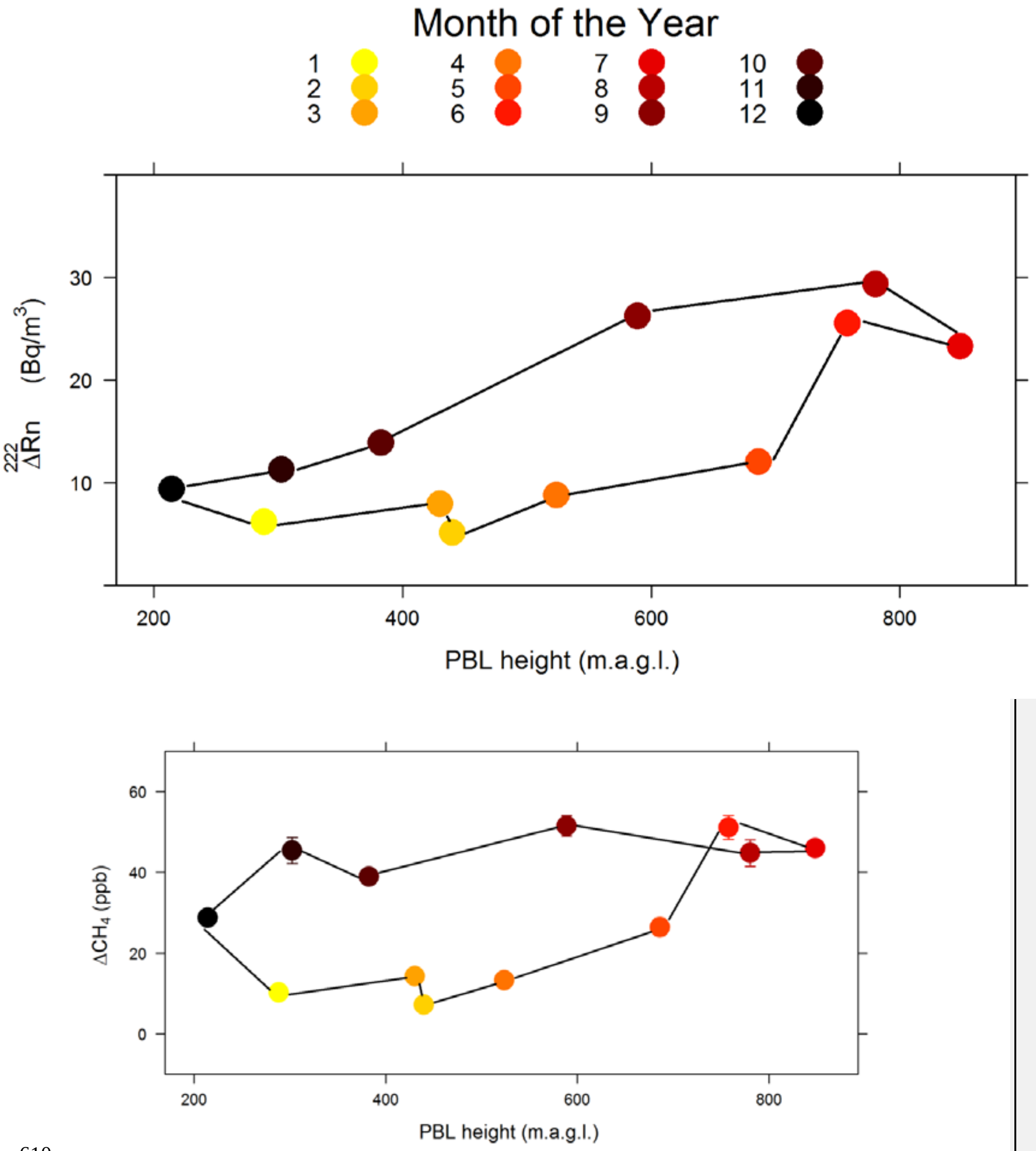

Formatted: Footer, Right

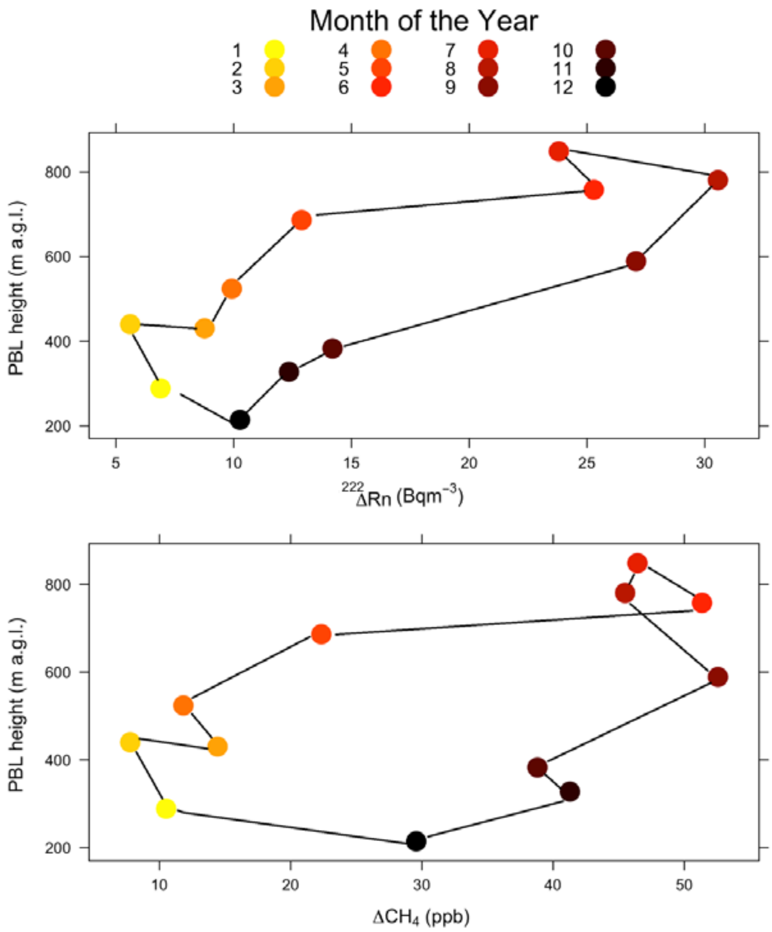

Figure ~~5~~6. Relation between monthly means of concentration amplitudes of ΔCH_4 (bottom panel) and $\Delta^{222}Rn$ (upper panel) measured during 2013-2015 at the GIC3 station and monthly ECMWF data of PBLH ~~at~~for the same area during same time interval.

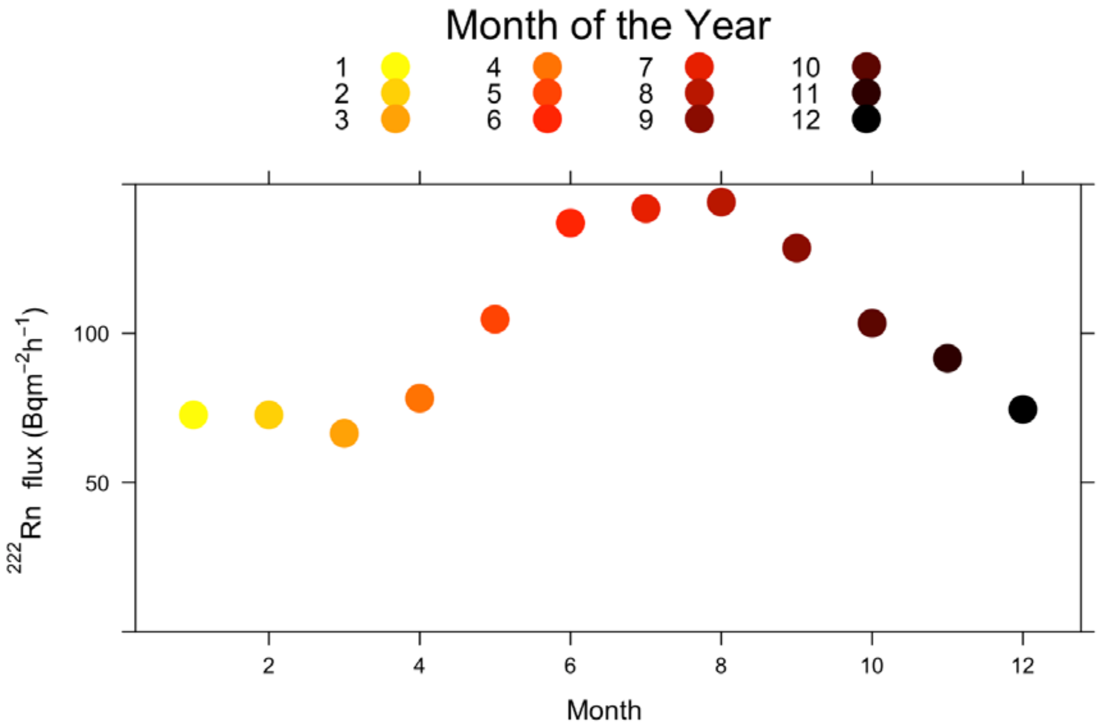

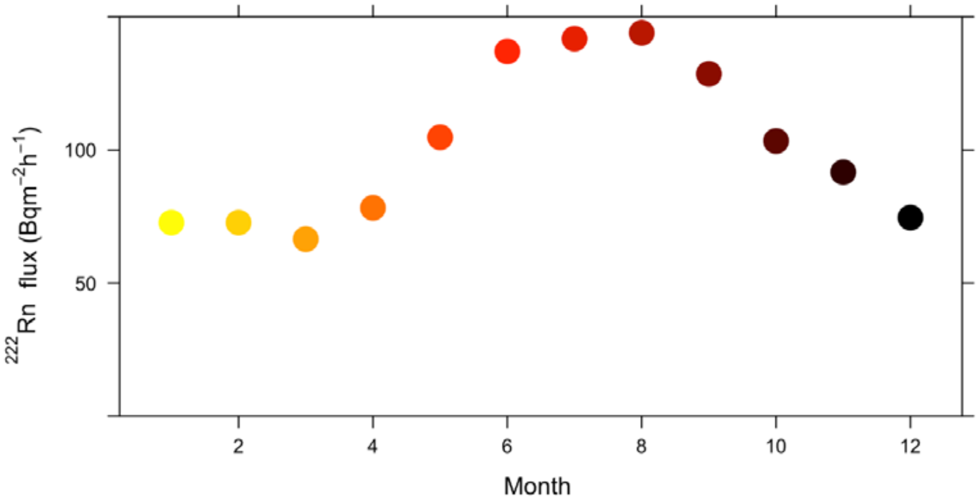

Figure ~~6~~7. Monthly ^{222}Rn flux means calculated by the UHU model and climatology for 2013-2015 at the GIC3 station. Coloured circles indicate the same months as in Figure 6.

Formatted: Footer, Right

3.4 Variations of CH_4 fluxes

Formatted: Font: Bold

So far, daily variations for both CH_4 mixing ratio and ^{222}Rn concentrations can be mainly explained in relation to the accumulation or dilution of gas concentration within the PBL. However, the hysteresis observed for the CH_4 mixing ratio of Figure 5 (bottom panel) seems to indicate a small change in the methane source between 12.00 UTC and 18.00 UTC.

Monthly $\Delta^{222}Rn$ variability can be understood when we account for seasonal ^{222}Rn flux changes. Unfortunately, existing emission inventories (EDGAR, 2010; MMA, 2016) ~~do~~ generally do not yet provide seasonally ~~and~~, hourly varying CH_4 emission values either for Europe in general ~~nor~~or for Spain in particular.

In order to understand the impact that temporal changes of CH_4 emissions may have on monthly mean atmospheric CH_4 ~~concentrations~~mixing ratios, we have ~~calculated nocturnal CH_4 fluxes. We have~~ applied two different methodologies, as explained in ~~the methodology section of this manuscript,~~Sections 2.4.1 and 2.4.2 and we have compared ~~the~~their resulting fluxes: ~~FLEXPART_RTM~~FR_CH_4 and ~~FLEXPART_EDGAR~~FE_CH_4, respectively. Figure ~~7~~8 presents the *effective* ^{222}Rn flux time series used for the application of the first methodology (RTM), together with the raw ^{222}Rn flux calculated by the UHU model and its seasonal climatology.

Formatted: Left

Formatted: Centered

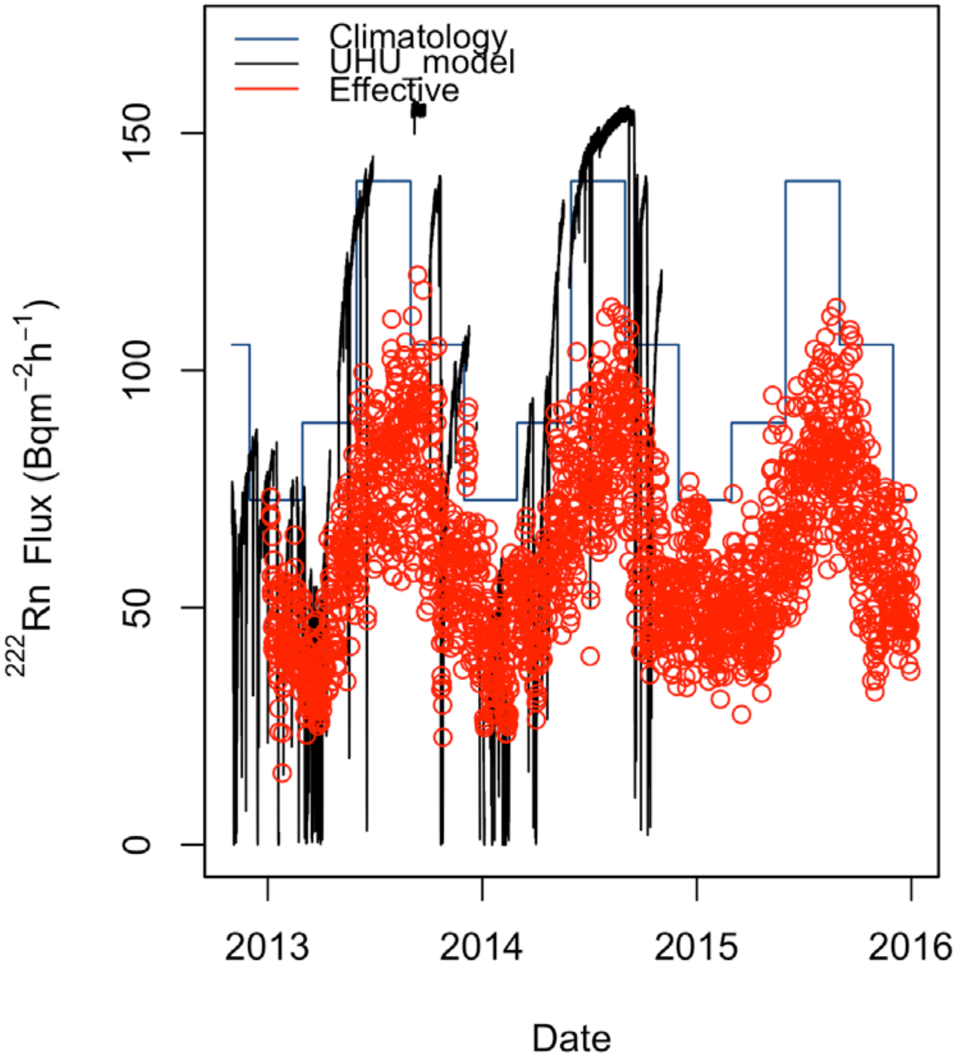

Formatted: Footer, Right

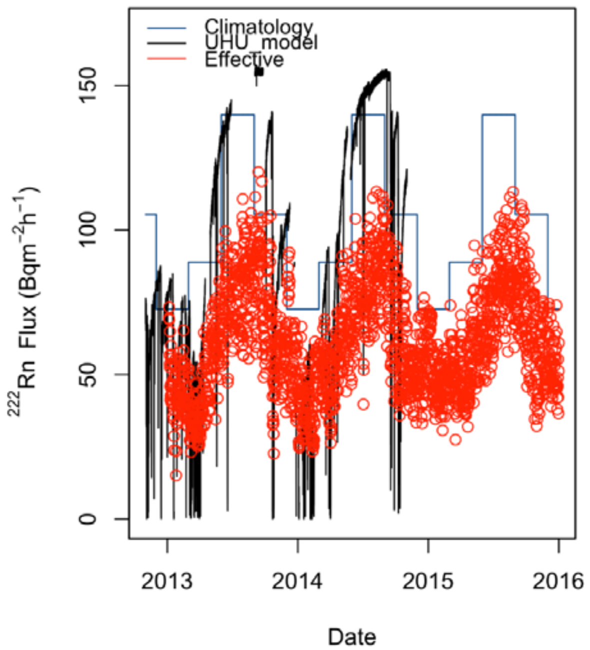

Figure ~~7~~8. Time series of local ^{222}Rn flux calculated by the UHU model (black line~~,~~; López-Coto et al.~~,~~. (2013~~)~~)) for the GIC3 area, ^{222}Rn flux seasonal climatology (blue line) and *effective* ^{222}Rn flux calculated on the basis of FLEXPART footprints (red dots). This last series was used within the RTM method.

Figure ~~8~~9 presents the time series of CH_4 fluxes estimated at the GIC3 station and T_i (grey shaded rectangles) indicates the time when transhumant livestock returns to the GNP after spending the winter in the south of Spain (Tapias, 2014; Rodríguez, 2015). The green shaded areas indicate the periods, between June and December, when transhumant livestock typically stays in the GIC3 region (Ruiz Perez and Valero Sáez, 1990; López Sáez et al., 2009; Libro Blanco, 2013). ~~The mean FLEXPART_RTM_CH4 flux is of 0.11 mg CH4 m-2 h-1 with a 25th and 75th percentiles of 0.07 mg CH4 m-2 h-1 and 0.14 mg CH4 m-2 h-1, respectively.~~ Data coverage in the second part of the time-series (2014-2015) is ~~significantly~~ higher than in the first period (2013-2014) because the simultaneous availability of ^{222}Rn and CH_4 data was higher. ~~FLEXPART_EDGAR~~The mean of FR_CH_4 fluxes ~~are higher,~~over the dataset is 0.11 mg CH_4 m^{-2} h^{-1} with ~~an annual mean value of~~ 25th and 75th percentiles of 0.07 mg CH_4 m^{-2} h^{-1} and 0.14 mg CH_4 m^{-2} h^{-1}, respectively. The mean of FE_CH_4 fluxes over the dataset is 0.33 mg CH_4 m^{-2} h^{-1} ~~and~~ with ~~a~~ 25th and 75th percentiles of 0.28 mg CH_4 m^{-2} h^{-1} and 0.36 mg CH_4 m^{-2} h^{-1}, respectively. ~~Furthermore, FLEXPART_EDGAR~~FR_CH_4 fluxes are constantly lower than FE_CH_4 fluxes, although this discrepancy decreases during some periods, as we will investigate later. FEC_CH_4 fluxes obtained with the EDGARv4.2 inventory by considering only the contribution of the cities that are located around the GIC3 station, in agreement with the masks presented in Table S1 of the supplement material, had a total mean value over the dataset of 0.02 mg CH_4 m^{-2} h^{-1} with ~~a 25th and 75th percentiles of 0 mg CH4 m-2 h-1~~25th and ~~0.01~~75th percentiles of 0 mg CH_4 m^{-2} h^{-1} and 0.006 mg CH_4 m^{-2} h^{-1}, respectively.

Formatted: Pattern: Clear (Yellow)

Formatted: Pattern: Clear (Yellow), Not Highlight

Formatted: Not Superscript/ Subscript

Formatted: Not Superscript/ Subscript

Formatted: Font: 10 pt, English (U.K.)

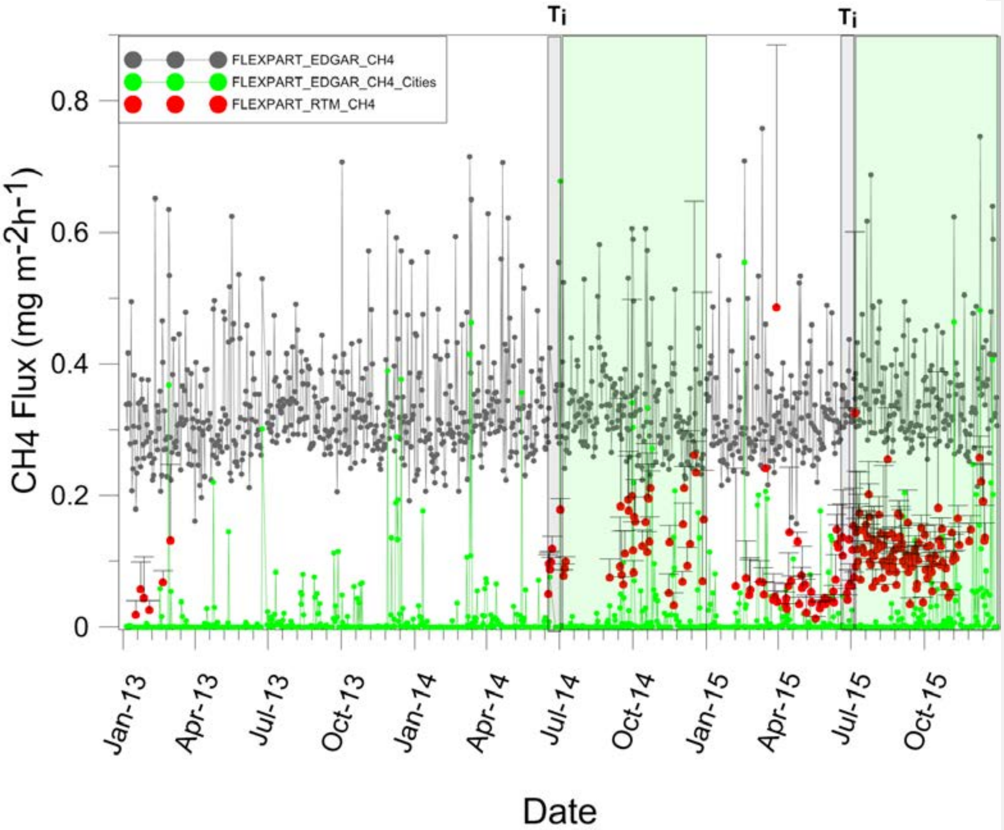

690

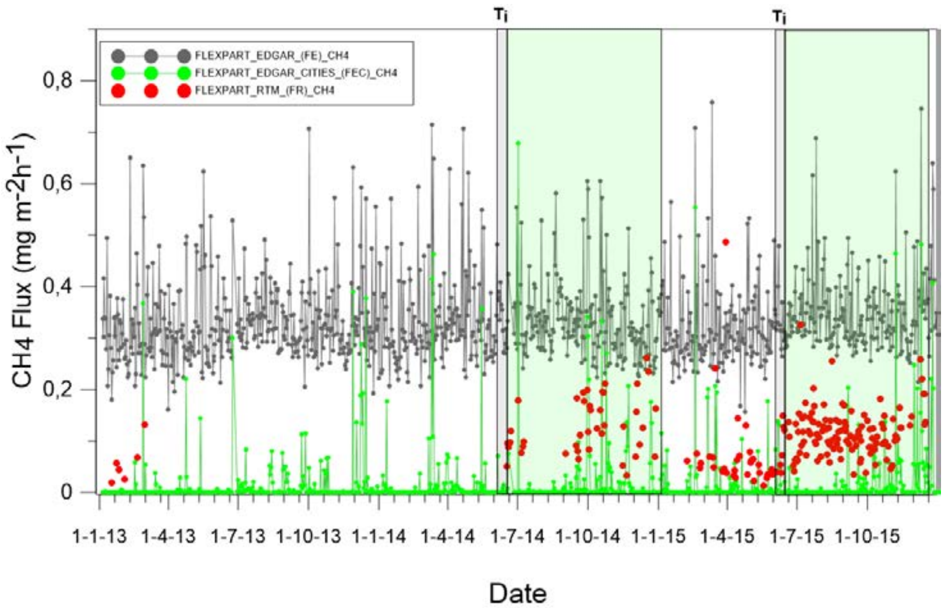

Formatted: Footer, Right

Figure ~~8~~9 Results of ~~nighttime FLEXPART_RTM~~night-time FR CH_4 fluxes (mg CH_4 m^{-2} h^{-1}) (red circles) obtained at the GIC3 station from January 2013 to December 2015 compared with ~~nighttime FLEXPART_EDGAR~~night-time FE CH_4 fluxes obtained using bottom-up inventory emissions (~~dark gray circles~~grey line) and calculated ~~FLEXPART_EDGAR~~FEC CH_4 fluxes from contributions from surrounding cities ~~contributions~~ (green circles). The weeks T_i ~~represents~~represent the period of 2014 (21st-27th June) and 2015 (20th-26th June~~), concurrent with the availability of FLEXPART_RTM_CH$_4$ fluxes data,~~) when transhumant livestock ~~came back~~returned to the GIC3 area after spending the winter in the south of Spain~~.~~ and concurrent with the availability of FR CH_4 fluxes data. Shaded green regions represent the ~~orientative~~ periods when transhumant livestock ~~stay~~remain in the GIC3 area.

Formatted: Font: Italic

Figure ~~9~~10 shows monthly boxplots of ~~FLEXPART_EDGAR~~FE CH_4 and ~~FLEXPART_RTM~~FR CH_4 fluxes. Shaded areas are coloured according to the main local wind directions ~~arriving at~~reaching the GIC3 station at night. This classification is based on the results presented in Figure ~~S3~~S2 of the supplementary material, where monthly windrose plots for the GIC3 station between 2013-2015 are shown. We can observe that there is no ~~significant~~ variability in monthly ~~FLEXPART_EDGAR~~FE CH_4 flux values. ~~As CH$_4$ emissions in the underlying emission inventory (EDGAR V4.2) are constant in time annually this reveals that no large impact of seasonally changing footprints on regional CH$_4$ fluxes is to be expected.~~ In contrast, ~~FLEXPART_RTM~~FR CH_4 flux results show ~~a noticeable~~an increase of CH_4 fluxes between June and December that seems to be independent of the seasonally changing dominant wind directions. This increase is also uncorrelated with seasonally changing ^{222}Rn fluxes (~~Figures 6 and~~ Figure 7).

Formatted: Not Superscript/ Subscript

The seasonal change of CH_4 fluxes between the first and the second half of the year at GIC3 could ~~be~~ indeed be related to variations in ~~the~~ local CH_4 emissions. ~~In addition, the highest FLEXPART_RTM_CH$_4$ flux values were observed in December, which also coincides with an increase of winds coming from surrounding cities according to FLEXPART_EDGAR_CH$_4$ results (see FLEXPART_EDGAR_CH4_cities data in Figures 8 and 9). Overall, cities contribution~~ The period between June and December represents the time of year when transhumant livestock returns to the GNP.

The contribution of cities is only visible during certain months~~, especially when dominant wind conditions come~~ and it seems to be related with winds coming from the ~~East~~east in the direction of the Madrid urban area (see Figure ~~S3~~S2 of the supplement material). ~~During the second semester of the year the difference between FLEXPART_RTM_CH$_4$ and FLEXPART_EDGAR_CH$_4$ fluxes is significantly reduced.~~

~~Finally, Figure 10 shows the boxplot of FLEXPART_EDGAR_CH$_4$ and FLEXPART_RTM_CH$_4$ fluxes aggregated according to the "cold" season, when there is no livestock in the GIC3 area, and "warm" season, when the animals are back to the valley. According to these data FLEXPART_RTM_CH$_4$ fluxes show an increase of around 0.05 mg CH$_4$ m^{-2} h^{-1} between "cold" and "warm" seasons.~~

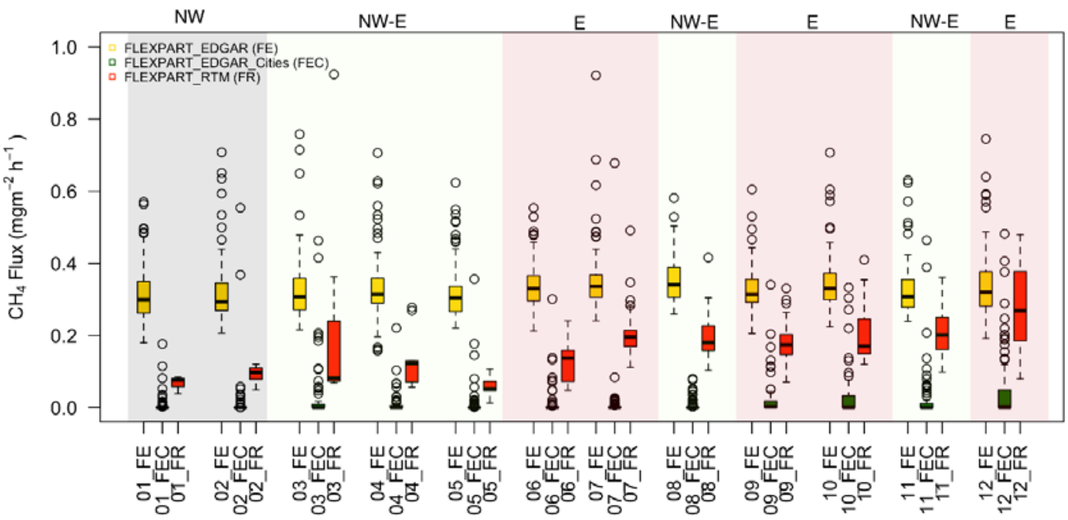

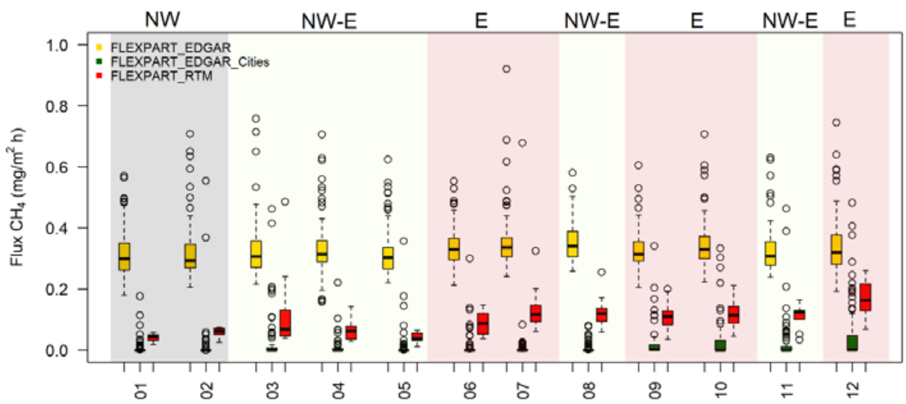

Figure ~~9. Boxplot~~10 Boxplots of monthly CH_4 fluxes (~~mgCH$_4$~~mg CH_4 m^{-2} h^{-1}) calculated ~~at~~for the GIC3 area using the RTM technique (red) and the EDGAR inventory (total in yellow; ~~cities~~ contribution of cities in green). Coloured areas indicate main wind directions for specific months. For each median (black bold line) the 25th (Q1; lower box limit) and 75th (Q3; upper box limit) percentiles are reported in the plot. The lower whisker goes from Q1 to the smallest non-outlier in the data set, and the upper whisker goes from Q3 to the largest non-outlier. Outliers are defined as >1.5 IQR or <1.5 IQR (IQR: Interquartile Range).

The disagreement observed between FE_CH_4 and FR_CH_4 fluxes in the months between June and December (Figures 9 and 10), when the transhumant livestock is in the GIC3 area, may be due to different reasons: i) a possible underestimation of the ^{222}Rn flux outputs from the UHU radon flux model, which would lead to lower FR_CH_4 fluxes (Equation 2). As explained previously, Karstens et al., 2015

Formatted: Not Superscript/ Subscript

Formatted: Footer, Right

compared their radon flux model with the UHU model and it gave, generally, 40 % higher ^{222}Rn flux values than the UHU model over Europe; ii) the methodology used within the EDGAR for the spatial disaggregation of national sector emission over the country could lead to a distribution of CH_4 emission in the GIC3 region higher than true levels leading to an overestimation of the FE_CH_4; iii) the fixed height of 300 m used for the calculation of nocturnal footprints could introduce a bias. However, this value is well within the range of nocturnal PBLH values calculated with data extracted from the ECMWF-HRES model. Furthermore, the calculated FLEXPART footprints were used both for FR_CH_4 and FE_CH_4 calculations and this should not affect the relative differences between their values.

When applying a 40% increase for the local ^{222}Rn source, as suggested by Karstens et al., 2015, we can re-calculate FR_CH_4 emissions as FR_CH_4_rescale. The boxplot of the monthly medians of FE_CH_4, FR_CH_4 and FR_CH_4 rescale are compared in Figure 11. The mean of FR_CH_4 rescale fluxes over the dataset is 0.29 mg CH_4 m^{-2} h^{-1} with 25th and 75th percentiles of 0.17 mg CH_4 m^{-2} h^{-1} and 0.34 mg CH_4 m^{-2} h^{-1}, respectively. FR_CH_4 rescale is in agreement with FE_CH_4 fluxes during the months between June and December, when the transhumant livestock remains in the GIC3 area (Cattle season).

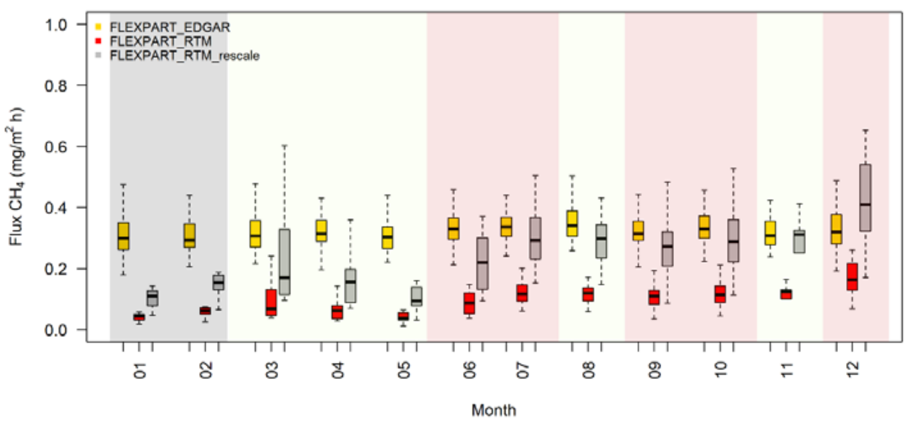

Figure 11, Boxplots of monthly CH_4 fluxes (mg CH_4 m^{-2} h^{-1}) calculated for the GIC3 area using the RTM technique (red), the EDGAR inventory (yellow) and RTM technique using the ^{222}Rn flux comparison factor found by Karstens et al., 2015 (grey). Coloured areas indicate main wind directions for specific months. For each median (black bold line) the 25th (Q1; lower box limit) and 75th (Q3; upper box limit) percentiles are reported in the plot. The lower whisker goes from Q1 to the smallest non-outlier in the data set, and the upper whisker goes from Q3 to the largest non-outlier. Outliers are defined as >1.5 IQR or <1.5 IQR (IQR: Interquartile Range).

Formatted: Tab stops: 1.27 cm, Left

Formatted: Pattern: Clear, Tab stops: 1.27 cm, Left

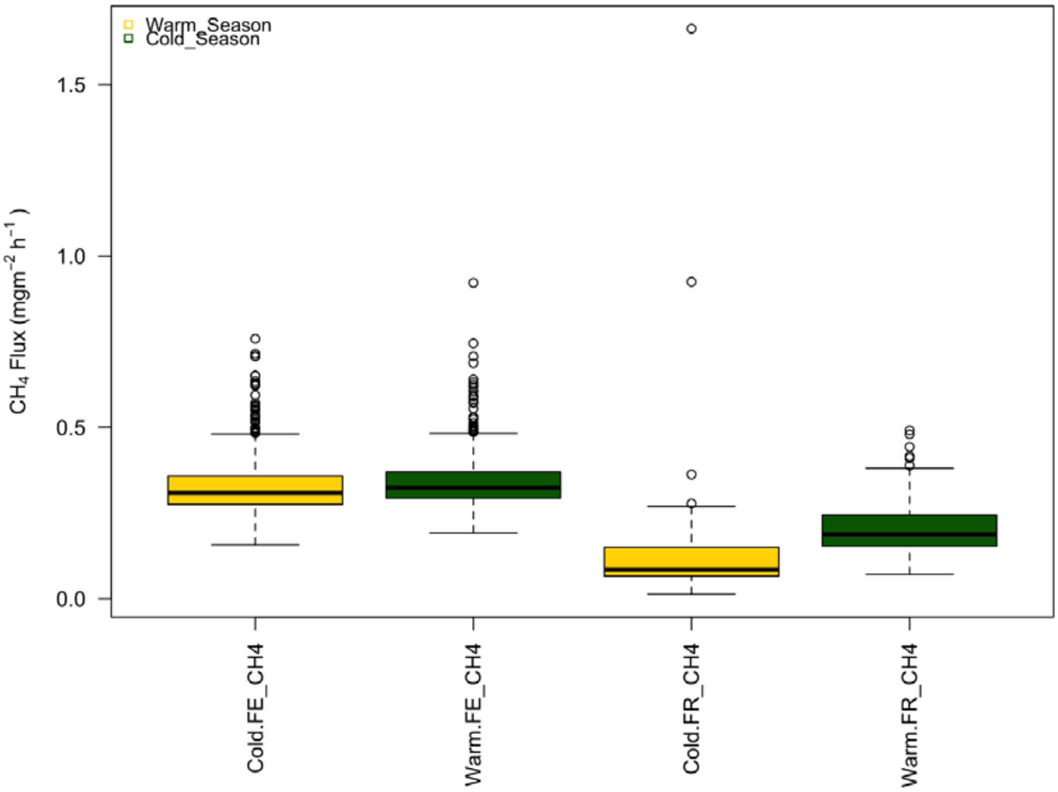

~~Figure 10. Boxplot of FLEXPART_EDGAR_CH_4 (FE) and FLEXPART_RTM_CH_4 (FR) fluxes (both in mg m^{-2} h^{-1}) calculated at GIC3 area during the "warm" season (June-December, dark green box) and the "cold" season (January-May, yellow box).~~

To highlight seasonal differences, FE_CH_4, FR_CH_4 and FR_CH_4_rescale fluxes are aggregated into two boxplots in Figure 12, according to the No-Cattle season (January until May), when there is no livestock in the GIC3 area, and Cattle season (June until December). According to these data during the No-Cattle season, FR_CH_4 fluxes present a mean value of 0.09 CH_4 m^{-2} h^{-1} with a standard deviation of 0.15 mg CH_4 m^{-2} h^{-1}. During the Cattle season, the mean value of FR_CH_4 fluxes is 0.12 CH_4 m^{-2} h^{-1} with a standard deviation of 0.05 mg CH_4 m^{-2} h^{-1}. The mean value of FR_CH_4_rescale fluxes is 0.24 mg CH_4 m^{-2} h^{-1} during the No-Cattle season with a standard deviation of 0.39 mg CH_4 m^{-2} h^{-1} and it is 0.30 mg CH_4 m^{-2} h^{-1} during the Cattle season with a standard deviation of 0.12 mg CH_4 m^{-2} h^{-1}. The corresponding values for FE_CH_4 fluxes are 0.31 mg CH_4 m^{-2} h^{-1} for the No-Cattle season and 0.32 mg CH_4 m^{-2} h^{-1} for the Cattle season.

Formatted: Footer, Right

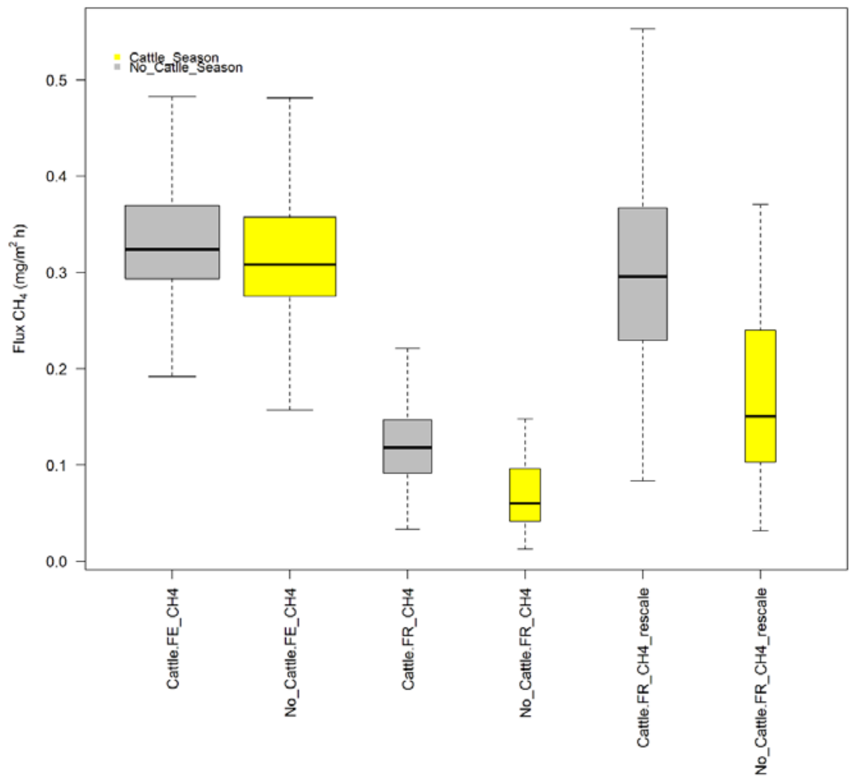

Figure 12. Boxplots of FE_CH_4, FR_CH_4 and FR_CH_4_corr fluxes (in mg m^{-2} h^{-1}) calculated for theGIC3 area during the "warm" season (June-December, yellow box) and the "cold" season (January-May, grey box). For each median (black bold line) the 25th (Q1; lower box limit) and 75th (Q3; upper box limit) percentiles are reported in the plot. The lower whisker goes from Q1 to the smallest non-outlier in the data set, and the upper whisker goes from Q3 to the largest non-outlier. Outliers are defined as >1.5 IQR or <1.5 IQR (IQR: Interquartile Range).

4 Discussion

The present results show the different influences that ~~both~~ meteorological conditions (PBLH and wind direction) and regional ~~fluxes influence~~sources may have on the variability of atmospheric CH_4 concentrations observed at the GIC3 station. ^{222}Rn observations have been used, together with modelled PBLH data, to better understand the reasons ~~of~~for the variability of the atmospheric CH_4 concentrations observed at ~~GIC3 and it has been shown they are really useful~~the station for different times scales. The use of ^{222}Rn as a tracer to ~~obtain~~calculate independent ~~estimates~~fluxes of GHGs ~~fluxes which can~~ has been shown in order to help ~~to improve~~with the improvement of emission inventories on a regional scale.

4.1 Daily variability of atmospheric CH_4 concentrations

Formatted: Tab stops: 1.27 cm, Left

Formatted: Font: 10 pt, Bold, English (U.K.)

Formatted: Left

Formatted: Font: 10 pt, Bold, English (U.K.)

Formatted: Font: 10 pt, Bold, English (U.K.)

The daily cycle of atmospheric CH_4 ~~concentrations~~mixing ratios (Figure 3a) measured at GIC3 shows ~~a~~ significant ~~variation~~changes between daytime and ~~nighttime~~night-time periods. The large increase of nocturnal CH_4 ~~concentrations~~mixing ratios can mainly be explained by the ~~significantly~~ decreased height of the planetary boundary layer (Figure ~~4~~4a), which is supported by a similar behaviour of ^{222}Rn concentrations~~.~~ (Figure 3c). Indeed, CH_4, as well as ^{222}Rn, reach their maximum concentration ~~values during the night~~ when the PBLH is ~~under 200~~below 300 m a.g.l. ~~and~~during the night, while their atmospheric concentrations decrease with the increase of the PBLH during daytime.

Formatted: English (U.S.)

The~~ good~~ correlation of PBLH and ^{222}Rn (and CH_4) in Figure ~~4~~5 indicates that ^{222}Rn ~~and CH_4~~ fluxes do not strongly vary on daily time-scales or, at least, not to a degree that ~~significantly influences~~ can influence their atmospheric concentration variability. ~~Nevertheless, average~~CH_4 fluxes seem to change on a daily time-scale. Average afternoon CH_4 concentrations are slightly enhanced compared to those from the morning for similar PBLH values (Figure ~~4~~5, bottom panel). They show a ~~small~~ hysteresis behaviour which could indicate ~~that~~ local emissions ~~slightly~~ increase ~~then,~~ or that a systematic transport of CH_4 enhanced air-masses~~ occur~~, not rich in radon, occurs at GIC3~~ during~~. Some studies (e.g. Bilek et al. 2001, Wang et al., 2015) have found strong emission increases of dairy cows post-feeding in feedlots, while McGinn et al. (2010) only found small diurnal increases of CH_4 emissions between 11h and 17h for grazing cattle. Unfortunately, no detailed information about the ~~afternoon~~feeding cycle of the GIC3 livestock is available, but grazing should be considered the predominant form of livestock management in transhumance. On the other hand, Figures 9 and 10 together with Figure S4 show the influences of eastern winds, coming from the Madrid direction, on the CH_4 fluxes.

Formatted: Normal, Left, Line spacing: single

Formatted: English (U.S.)

Formatted: English (U.S.)

4.2 Seasonal variability of atmospheric CH_4 concentrations

Formatted: Font: 10 pt, Bold, English (U.K.)

To understand the ~~impact~~drivers of monthly changing concentrations of CH_4 we need to account for PBLH~~,~~ local meteorology~~ and~~, changing regional emissions~~, the interpretation of monthly data needs to account also for the~~ and changing background concentrations of CH_4 at GIC3. ~~To take this issue into account, we discuss the mean monthly local enhancement of CH_4 (ΔCH_4) between~~Median monthly mixing ratios for daytime and ~~nighttime. This definition of ΔCH_4~~night-time (Figure 3b) are discussed alongside ΔCH_4 (Figure 6) which allows us to subtract seasonal and synoptic background variations~~, and~~. This enables us to focus on the impact of PBLH for individual days that are then averaged to investigate how ΔCH_4 changes on a monthly basis. The observed variability of ΔCH_4 (~~Figure 5, lower panel~~Figures 3b and 6) cannot be explained only in terms of ~~the~~ changes of the PBLH. Monthly averages of ΔCH_4 (and night-time monthly CH_4 boxplots, Figure ~~2~~3b) present their maximum values between June and December; and their minimum values during the rest of the months ~~independently~~irrespective of the height of the PBL.

Formatted: Not Superscript/ Subscript

Formatted: Footer, Right

From co-located ^{222}Rn concentration observations we learn that ~~a significant~~an increase in the ~~regional~~average monthly fluxes (Figure ~~6~~7) can compensate the effect of increased dilution in the deeper summer PBL on the observed concentrations (Figure ~~5).~~6, upper panel) yielding similar atmospheric ^{222}Rn concentrations. The increase of the modelled ^{222}Rn flux in the GIC3 region from the winter to ~~summer~~autumn season and the following decrease can coherently help to explain the variation observed in monthly Δ^{222}Rn. ~~The~~Thus, the comparison between ΔCH_4 and Δ^{222}Rn suggests ~~to us~~ that there may ~~be~~ also be a ~~strongly varying seasonal source~~monthly variability in the sources of CH_4 which should help to understand monthly atmospheric mixing ratios variability. This has been further confirmed by our ~~FLEXPART_RTM~~FR_CH_4 ~~fluxes~~flux estimates, as seen in Figures ~~8,~~ 9, 10 and ~~10~~11. Of course, the ~~FLEXPART_RTM~~FR_CH_4 ~~fluxes~~flux estimates are limited to ~~nighttime, but, as previously discussed in section 4.1, we can assume that the daily~~night-time due to the RTM hypothesis. FR_CH_4 fluxes show a total mean value 33% lower than FE_CH_4 fluxes over the data set. When ^{222}Rn fluxes ~~of CH_4 only vary to a small degree and we thus consider that the nocturnal RTM results~~ are ~~representative for the overall daily CH_4 fluxes.~~rescaled according to Karstens et al., 2015, this difference is drastically reduced to 10-15%.

~~FLEXPART_~~RTM~~-~~-based CH_4 fluxes show an increase of 25% during the second semester of the year~~.~~ ~~The~~ on a monthly basis. This increase ~~seems to coincide~~coincides with the period of the year when transhumant livestock resides in the GIC3 region. ~~UPA (2009) reports that around 40,000~~ Although no exact information is available on the number of animals~~, mainly bovine, crossed the Puerto del Pico border of the Sierra de Gredos in June 2014 and June 2015 coming back after the winter. During~~ present only in the GIC3 area, during this period of enhanced ruminant emissions, ~~FLEXPART_RTM_CH_4 and FLEXPART_EDGAR~~ the difference between CH_4 fluxes ~~are much more in agreement indicating that~~ based on RTM and the ~~differences observed~~EDGAR inventory is reduced from ~~January~~73% to 65% for FR_CH_4 and from 27% to ~~May could be caused by~~9% for FR_CH_4_rescale The difference during the No-Cattle season is likely due to the constant annual emission factor of CH_4 ~~in the~~emission used within the bottom-up inventory which, of course, cannot yet reflect ~~this process (~~transhumance~~) in the annual mean~~ activity. The likely explanation is that all emissions ~~inventory.~~from the aforementioned animals has been constantly allocated to this region, which is why FE_CH_4 is also larger than FR_CH_4_rescale during months when they are not present. The RTM analysis performed here ~~allows to observe the additional contribution to the regional~~ suggests that transhumance could be a relevant process to understand sub-annual CH_4 emissions ~~due to livestock activity in the GIC3 area, which appears to be a dominant source in the second half of the year. From Figure 10, livestock seems to add on a monthly basis around 0.05 mgCH_4 m^{-2} h^{-1} during their residence at GIC3 area,~~in the region and ~~an annual contribution~~can affect the spatial distribution of ~~29% to the~~CH_4 sources within a country. Our study, indicates that the choice of ^{222}Rn model has an important impact on annual total ~~regional CH_4 flux~~emissions calculated, while seasonal and short-term patterns are preserved.

5 Conclusions and outlook

Formatted: Font: 10 pt

Formatted: Font: 10 pt, English (U.K.)

Formatted: Font: 10 pt, English (U.K.)

Formatted: Font: 10 pt, Bold, English (U.K.)

To gain a full picture of the Spanish (and European) GHGs balance ~~the~~, understanding of CH_4 emissions in ~~the currently understudied~~different regions is a critical challenge as well as is the improvement of bottom-up inventories for all European regions. Our study uses, among others, GHGs, meteorological and ^{222}Rn tracer data from one of the eight ~~ClimaDat~~ stations of the new ClimaDat network in Spain, which provides ~~important new~~ continuous atmospheric observations of CH_4 and ^{222}Rn in a ~~systematically under-sampled~~ region of ~~central Spain.~~Europe. The present study underlines the fact that this data, combined with retrieved PBLHs data~~,~~ and atmospheric transport modelling (~~FLEXPARTv6.2) and a bottom-up emission inventory (EDGARv4.2), allows addressing~~FLEXPARTv92) can help to understand the main causes of ~~the spatial and~~ temporal variability of ~~the~~GHG mixing ratios and can offer new insights into regional ~~GHGs sources.~~

~~From our joint interpretation of atmospheric CH_4 and ^{222}Rn concentrations we can conclude that the concurrent observations of ^{222}Rn permitted us to see more clearly the impact of PBLH on the variability of atmospheric concentrations on daily basis. ^{222}Rn data also allowed us to implement the Radon Tracer Method (RTM) to observe seasonal CH_4 flux variability. This can be useful to help improve bottom-up inventories of CH_4 from hard to tackle~~emissions by identifying the impacts of changing sources, e.g. ~~agriculture, especially in relation to their temporal variations.~~emissions from transient livestock.

These first promising results ~~motivate the~~ should lead to further application of this RTM to other ~~GHGs~~GHG time series from the ClimaDat network~~, as well as~~ and potentially in continent-wide networks such as ICOS that routinely perform co-located ~~GHGs~~GHG and ^{222}Rn observations. Particularly, the use of the RTM has been shown, while also highlighting the need to improve this method, especially in regard to: i) validation of the ^{222}Rn flux maps applied within the RTM; ii) standardization of the footprint calculation.

~~Although~~ Although the transhumant livestock seems to be the likely reason for the seasonal changes observed in the FR CH_4 fluxes at the GIC3 station, other sources could also contribute to this seasonality such as waterbodies or other natural emissions. These previous sources are not included in the EDGAR inventory, but they could be detected by the RTM. However, those sources would not be able to fully explain the sudden onset of increased RTM-based CH_4 fluxes but would rather contribute to a slow increase in warmer months. Further research applying isotopic analysis of CH_4 mixing ratios measured at the GIC3 station for the different seasons should be carried out, as well as transects of the regions to assess the impact of natural sources on CH_4 mixing ratios. In addition, no precise data on transhumant activity in Spain is available ~~so far,~~to date, but our study ~~highlights the importance of transhumance, as an anthropogenic activity for livestock management, in the regional CH_4 budget of central Spain. Establishing a clear~~suggests the existence of a link between regional CH_4 fluxes and highlights the need for more information of transhumance activity ~~will allow accounting for this effect~~which could be taken into account in future emission inventories of ~~the~~this region (and Europe). In addition, our results show that urban emissions can be transported and could influence the atmospheric composition of remote rural areas over several hundred kilometres~~.~~

Formatted: Font: 10 pt, English (U.K.)

Formatted: Font: 10 pt, English (U.K.)

Formatted: Footer, Right

~~Besides supporting better future temporal information for inventories, our findings could also be applied to monitor the impact of emission mitigation strategies on regional emission trends. Indeed, other researchers suggested that Best Management Practices (BMP) for cattle can drive a reduction of 22-30% in CH_4 emissions compared with continuous grazing management (De Ramus et al., 2003; FAO 2013). In this sense, the methodology applied in this study could be useful in the future to observe the impact of BMP on the reduction of ruminant CH_4 emissions on a regional scale. A decrease of CH_4 emissions, if such mitigation strategies are applied widely, can furthermore have positive impacts on regional climate and air quality in different regions of the world.~~

~~We think that to understand long-term (inter-annual) CH_4 concentration changes on global and continental scales, studies focusing on better understanding CH_4 sources on a regional scale, such as our work, provide an important piece to the puzzle.~~ under specific synoptic conditions.

Formatted: Font: 10 pt, English (U.K.)

Formatted: Font: Not Bold

Acknowledgements

Formatted: Font: 10 pt, English (U.K.)

The ~~authors thank the funding~~ research leading to these results has received ~~by: Obra Social "La~~funding from "la Caixa" ~~to finance~~Foundation.with the ClimaDat ~~Project~~project (2010-2014~~);~~) and from the Ministerio Español de Economía y Competividad, Retos 2013 (2014-2016) with the MIP (Methane interchange between soil and air over the Iberian Península) project (reference: CGL2013-46186-R~~)~~ ~~funded by Ministerio Español de Economía y Competividad, Retos 2013, 2014-2016~~). This study was also made possible thank to collaboration with the Autonomous Community of Castile and León and the Sierra de Gredos Regional Park.

Formatted: Font: 10 pt, English (U.K.)

C. G. particularly thanks the Ministerio Español de Educación, Cultura y Deporte ~~to~~for partially ~~support~~supporting her work with the research mobility grant "José Castillejos" (ref. CAs15/00042). The research of F.R.V. ~~is~~Has been funded and supported by the Chaire industrielle BridGES, a joint research program between ThalesAleniaSpace, Veolia and the parent institutions of LSCE (CEA, CNRS, UVSQ).

Formatted: Font: 10 pt, English (U.K.)

~~Authors~~The authors warmly thank: i) the LAO (Atmosphere and Ocean laboratory) team, in the persons of: Rosa Arias, Manel Nofuentes, Oscar Batet, Lidia Cañas, Silvia Borras, Paola Occhipinti and Eusebi Vazquez, for their efforts in the installation, maintenance and calibration of all IC3 climatic stations and data, including the GIC3 station, where this study has been performed; ii) the INTE team, in the persons of: Vicente Blasco and Juan Antonio Romero, for their work in the building of the ARMON installed at the GIC3 station; iii) Albert Jornet, software engineer of the IC3 who developed, together with Roger Curcoll, an automatic system for the daily running of FLEXPART backward simulations; iv) ~~the Weather Forecasting Service of~~ Dr. Israel Lopéz-Coto and the University of Huelva~~, (http://atmos.uhu.es/)~~ for ~~providing access to~~ the ~~WRF simulations database and~~ radon flux modelled data; v) Dr. Stefano

Formatted: Not Highlight

Formatted: Not Highlight

Formatted: Not Highlight

Formatted: Not Highlight

Formatted: Not Highlight

Formatted: Not Highlight

Formatted: Not Highlight

Galmarini for helping to improve the ~~computing resources used on the Radon emissions calculations. Authors also thank~~manuscript; vi) David Carslaw and Karl Ropkins, developers of the R package OpenAir (www.openair-project.org), used in the present work for data analysis~~. Finally, authors appreciate~~; vi) the ~~editor and~~ two anonymous reviewers for their comments and suggestions ~~which help in the improvement of this~~for improving our work.

Formatted: Font color: Black, English (U.S.), Not Highlight

Formatted: Font color: Black, English (U.S.), Not Highlight

Formatted: Font color: Black, English (U.S.)

Formatted: Internet Link, Font: 12 pt

~~References~~

~~Àgueda, A., Grossi, C., Pastor, E., Rioja, E., Sánchez-García, L., Batet, O., Curcoll, R., Ealo, M., Nofuentes, M., Occhipinti, P., Rodó, X., Morguí, J. A: Temporal and spatial variability of ground level atmospheric methane concentrations in the Ebro River Delta. In Press in Atmos. Pollution Res., doi: 10.1016/j.apr.2017.01.009, 2017.~~

~~Arnold, D., Vargas, A., Vermeulen, A., T., Verheggen, B., Seibert, P.: Analysis of radon origin by backward atmospheric transport modelling. Atmos. Environ 44, 494-502, doi: 10.1016/j.atmosenv.2009.11.003, 2010.~~

~~Bergamaschi, P., Krol, M., Meirink, J.F., Dentener,F., Segers, A., van Aardenne, J., Monni, S., Vermeulen, A.T., Schmidt, M., Ramonet, M., Yver, C., Meinhardt, F., Nisbet, E.G., Fisher, R.E., O'Doherty, S., Dlugokencky, E.J.: Inverse modelling of European CH_4 emissions 2001-2006. J. Geophys. Res., 115, D22309, doi: 10.1029/2010JD014180, 2010.~~

~~Crosson, E.R.: A cavity ring-down analyzer for measuring atmospheric levels of methane. Carbon dioxide and water vapor. Appl. Phys. B 92, 403–408, doi: 10.1007/s00340-008-3135-y, 2008.~~

~~De Ramus, H.A., Clement, T.C., Giampola, D.D., Dickison, P. C.: Methane Emissions of Beef Cattle on Forages: Efficiency of Grazing Management Systems. J. Environ. Qual. 32, 269-277, doi: 10.2134/jeq2003.2690, 2003.~~

~~EDGAR: Emission Data Base for Global Atmospheric Research release version 4.1 of the European Commission. Joint Research Center (JRC)/Netherland Environmental Assessment Agency (PBL). Available: http://edgar.jrc.ec.europa.eu/index.php#, 2010.~~

~~European Center for Medium Range Weather Forecasting: Diagnostic boundary layer height, in IFS Documentation CY31r1, vol. 4, Physical Processes, Reading, U. K. (Available at:~~

Formatted: Footer, Right

~~http://www.ecmwf.int/sites/default/files/elibrary/2007/9221-part-iv-physical-processes.pdf), 2006.~~

~~EEA, 2007. European Environment Agency CORINE Land Cover. Corine Land Cover technical guide. http://www.eea.europa.eu/publications/tech40add.~~

~~FAO: The State of Food Insecurity in the World 2013. The multiple dimensions of food security. Source: http://www.fao.org/docrep/018/i3434e/i3434e.pdf. Rome, FAO, 2013.~~

~~Font, A., Grimmond, C.S.B., Morguí, J.A., Kotthaus, S., Priestman, M., Barratt, B.: Cross-validation of inferred daytime airborne CO_2 urban-regional scale surface fluxes with eddy covariance observations and emissions inventories in Greater London. Atmos. Chem. Phys. Discuss., 13, 13465-13493, doi: 10.5194/acpd-13-13465-2013, 2013.~~

~~Griffiths, A.D., Parkes, S.D., Chambers, S.D., McCabe, M.F., Williams, A.G.: Improved mixing height monitoring through a combination of lidar and radon measurements. Atmos. Meas. Tech., 6, 207-218, doi: 10.5194/amtd-5-6835-2012, 2012.~~

~~Grossi, C., Arnold, D., Adame, J. A., López-Coto, I., Bolívar, J.P., de la Morena, B.A., Vargas, A.: Atmospheric ^{222}Rn concentration and source term at El Arenosillo 100 m meteorological tower in southwest Spain, Radiat. Meas., 47(2), 149–162, doi: 10.1016/j.radmeas.2011.11.006, 2012.~~

~~Grossi, C., Vogel, F.R., Morguí, J.A., Curcoll, R., Àgueda, A., Batet, O., Nofuentes, M., Occhipinti, P., Vargas, A., Rodó, X.: First estimation of CH_4 fluxes using the ^{222}Rn tracer method over the central Iberian Peninsula, in Air Pollution XXII, WIT Transactions on Ecology and the Environment, 183, 233-245, doi: 10.2495/AIR140201, 2014.~~

~~Grossi, C., Àgueda, A., Vogel, F.R., Vargas, A., Zimnoch, M., Wach, P., Martín, J.E., López-Coto, I., Bolívar, J.P., Morguí, J. A., Rodó, X.: Analysis of ground-based 222Rn measurements over Spain: filling the gap in south-western Europe. J. Geophys. Res. Atm., 121, doi: 10.1002/2016JD025196, 2016.~~

~~Hammer, S., Levin, I.: Seasonal variation of the molecular hydrogen uptake by soils inferred from continuous atmospheric observations in Heidelberg, southwest Germany. Tellus B 61,3, 556-565, doi: 10.1111/j.1600-0889.2009.00417.x, 2009.~~

~~Hernández, M.A.: Ávila concentra el 85% de la ganadería trashumante que pervive en España. Source: cadenaser.com/emisora/2016/04/18/ser_avila/1460979067_721996.html, 2916.~~

~~Hiller, R.V., Bretscher, D., DelSontro, T., Diem, T., Eugster, W., Henneberger, R., Hobi, S., Hodson, E., Imer, D., Kreuzer, M., Künzle, T., **Merbold, L.,** Niklaus, P.A., Rihm, B., Schellenberger, A., Schroth, M.H., Schubert, C.J., Siegrist, H., Stieger, J., Buchmann, N., Brunner, D.: Anthropogenic and natural methane fluxes in Switzerland synthesized within a spatially explicit inventory. *Biogeosciences* 11, 1941-1959, doi: 10.5194/bg-11-1941-2014, 2014.~~

~~IPCC (Intergovernmental Panel on Climate Change). Climate Change 2013: the physical science basis. In: Stocker, T.F., Qin, D., Plattner, G.K., Tgnor, M., Alle, S., Boshung, J., Nauels, A., Yu Xia, Bex, V., Midgley, P. editors. Contribution of working group I to the fifth assessment report of the Intergovernmental Panel on Climate Change. Available at: www.climatechange2013.org/images/uploads/WGIAR5_WGI12Doc2b_FinalDraft_All.pdf, 2013.~~

~~Jeong, S., Ying-Kuang, H., Andrews, A.E., Bianco, L., Vaca, P., Wilezak, J.M., Fischer, M.L.: A multitower measurement network estimate of California's methane emissions. J. Geophys. Res.: Atm. 118, 1-13, doi: 10.1002/jgrd.50854, 2013.~~

~~Levin, I., Hammer, S., Eichelmann, E., Vogel, F.R.: Verification of greenhouse gas emission reductions: the prospect of atmospheric monitoring in the polluted areas. Phil. Trans. R. Soc. A 369, 1906-1924, doi: 10.1098/rsta.2010.0249, 2011.~~

~~Libro Blanco: La trashumancia en España. Red rural nacional, Secretaría General de Agricultura y Alimentación. Dirección General de Desarrollo Rural y Política Forestal. Subdirección General de Modernización de las Explotaciones (source: www.magrama.gob.es/es/desarrollo-rural/publicaciones/publicaciones-de-desarrollo-rural/LIBRO_BLANCO_2013_tcm7-245950.pdf), 2013.~~

~~López-Coto, I., Mas, J.L., Bolívar, J.P.: A 40-year retrospective European radon flux inventory including climatological variability, Atmos. Environ., 73, 22–33, doi: 10.1016/j.atmosenv.2013.02.043, 2013.~~

~~López Sáez, J.A., López Merino, L., Sánchez, F.A., Pérez Díaz, S.: Contribución paleoambiental al studio de la trashumancia en el sector abulense de la Sierra de Gredos. Hispania LXIX, 231, 9-38, ISSN: 0018-2141, 2009.~~

~~MMA (Ministerio de Medio Ambiente). Inventario de emisiones de gases de efecto invernadero de España. Años 1990-2014. Comunicación al secretariado de la convención marco de NNUU sobre cambio climático. Secretaría General para la Prevención de la Contaminación y del Cambio Climático. Dirección General de Calidad y Evaluación Ambiental. Subdirección General de Calidad del Aire y Prevención de Riesgos, 1-1212, source: www.magrama.gob.es/es/calidad-y-evaluacion-ambiental/temas/sistema-espanol-de-inventario-sei-/nir_ed2016_def_tcm7-417776.pdf, Madrid, 2016.~~

Formatted: Footer, Right

~~Nazaroff, W.W., and Nero, A.V. (Eds.): Radon and its decay products in indoor air, John Wiley & Sons, New York, USA, doi: 10.1063/1.2810982, 1988.~~

~~NRC. Committee on Methods for estimating Greenhouse Gas Emissions of the National Research Council: Verifying greenhouse gas emissions. Washington (DC), The National Academic Press, 2010.~~

~~Prinn, R. G.: Measurement equation for trace chemicals in fluids and solution of its inverse. Geophysical Monograph Series, 3-8, doi: 10.1029/gm114p0003, 2000.~~

~~Rella, C.: Accurate Greenhouse Gas Measurements in Humid Gas Streams Using the Picarro G1301 Carbon Dioxide/Methane/Water Vapor Gas Analyzer; White Paper; Picarro Inc.: Sunnyvale, CA, USA, 2010.~~

~~Rodríguez, M.: Más de 400 reses trashumantes regresan a Gredos. Diario de Avila. 20/06/2015 (source: www.diariodeavila.es/noticia/ZB81ABF36-CC0C-2ABE-4545305C6871EB6E/20150621/mas/400/reses/trashumantes/regresan/gredos).~~

~~Ruiz Perez, M., Valero Sáez, A.: Transhumance with cows as a rational land use option in the Gredos Mountains (Central Spain). Human Ecology 18, 2, 187-202, doi: 10.1007/bf00889182, 1990.~~

~~Schery, S.D., Wasiolek, M.A.: Modeling Radon Flux from the Earth surface, in Radon and Thoron in the human environment. World Scientific Pubblishing, 207-217, doi: 10.2172/607500, 1998.~~

~~Schmidt, M., Graul, R., Sartorius, H., Levin, I.: Carbon dioxide and methane in continental Europe: a climatology, and ^{222}Radon-based emission estimates. Tellus 48B, 457-473, 1996.~~

~~Schmithüsen, D., Chambers, S., Fischer, B., Gilge, S., Hatakka, J., Kazan, V., Neubert, R., Paatero, J., Ramonet, M., Schlosser, C., Schmid, S., Vermeulen, A., Levin, I.: A European-wide ^{222}Radon and ^{222}Radon progeny comparison study, in Press in Atmos. Meas. Tech., doi:10.5194/amt-2016-111, 2016.~~

~~Seidel, D., Zhang, Y., Beljaars, A., Golaz, J. C. Jacobson, A., Medeiros, B.: Climatology of the planetary boundary layer over the continental United States and Europe. J. Geophys. Res., 117, D17106, doi: 10.1029/2012JD018143, 2012.~~

~~Skamarock, W. C., Klemp, J. B., Dudhia, J., Gill, D. O., Barker, D. M., Duda, M. G., Huang, X-Y., Wang, W., Powers, J.G.: A Description of the Advanced Research WRF Version 3, NCAR Technical Note, NCAR/TN-475+STR, 2008.~~

~~Stohl, A., Hittenberger, M., Wotawa, G.: Validation of the Lagrangian particle dispersion model FLEXPART against large scale tracer experiments. Atmos. Environ. 32, 4245-4264, doi: 10.1016/s1352-2310(98)00184-8, 1998.~~

~~Szegvary, T., Conen, F. Ciais, P.: European [222]Rn inventory for applied atmospheric studies, Atmos. Environ., 43(8), 1536–1539, doi: 10.1016/j.atmosenv.2008.11.025, 2009.~~

~~Tapias, R.M.: De Mombeltrán al puerto del Pico, con la vaca avileña. El Mundo. (Source: www.elmundo.es/madrid/2014/07/01/53b1a5d3e2704e99368b4585.html), Madrid, 01/07/2014.~~

~~Tohjima, Y., Kubo, M., Minejima, C., Mukai, H., Tanimoto, H., Ganshin, A., Maksyutov, H., Katsumata, K., Machida, T., Kita, K.: Temporal changes in the emissions of CH_4 and CO from China estimated from CH_4 / CO_2 and CO / CO_2 correlations observed at Hateruma Island. Atmos. Chem. Phys., 14, 1663–1677, doi: 10.5194/acp-14-1663-2014, 2014.~~

~~Troen, I., Mahrt, L.: A simple model of the atmospheric boundary layer: Sensitivity to surface evaporation, Boundary Layer Meteorol., 37, 129–148, doi:10.1007/BF00122760, 1986.~~

~~Van der Laan, S. Karstens, U. Neubert, R.E.M. Van der Laan-Luijkx, I.T. Meijer, H.A.J.: Observation-based estimates of fossil fuel-derived CO_2 emissions in the Netherlands using $\Delta^{14}C$, CO and [222]Radon. Tellus B (62-5), 389-402, doi: 10.1111/j.1600-0889.2010.00493.x, 2010.~~

~~Vargas, A., Arnold, D., Adame, J.A., Grossi, C., Hernández-Ceballos, M.A., Bolívar, J.P.: Analysis of the vertical radon structure at the Spanish “El Arenosillo” tower station, J. Environ. Radioact., 139, 1-17, doi: 10.1016/j.jenvrad.2014.09.018, 2015.~~

~~Vermeulen, A.T., Pieterse, G., Hensen, A., Van den Bulk, W.C.M, Erisman, J.W: COMET: a Lagrangian transport model for greenhouse gas emission estimation – forward model technique and performance for methane. Atmos. Chem. Phys. Discuss., 6, 8727-8779, doi: 10.5194/acpd-6-8727-2006, 2006.~~

~~Vogel, F.R., Ishizawa, M., Chan, E., Chan, D., Hammer, S., Levin, I., Worthy, D.E.J.: Regional non-CO_2 greenhouse gas fluxes inferred from atmospheric measurements in Ontario, Canada, J. Integr. Environ. Sci., 9(S1), 1-15, doi: 10.1080/1943815X.2012.691884, 2012.~~

~~Wada, A., Matsueda, H., Murayama, S., Taguchi, S., Hirao, S., Yamazawa, H., Moriizumi, J., Tsuboi, K., Niwa, Y., Sawa, Y.: Quantification of emission estimates of CO_2, CH_4 and CO for East Asia derived from~~

Formatted: Footer, Right

~~atmospheric radon-222 measurements over the western North Pacific, Tellus B, 65, 18037, doi: 10.3402/tellusb.v65i0.18037, 2013.~~

~~WWF (International World Wide Fund For Nature): Editor Barney Jeffries, Spanish version by Mar Rego, ISBN 978-2-940443-84-0, doi: d2ouvy59p0dg6k.cloudfront.net/downloads/informe_anual_wwf_2013_esp_1.pdf, 2014.~~

~~Zahorowski, W., Chambers, S.D.A., Henderson-Sellers, A.: Ground based radon-222 observations and their application to atmospheric studies, J. Environ. Radioact., 76(1-2), 3-33, doi: 10.1016/j.jenvrad.2004.03.033, 2004.~~

~~Zimnoch, M., Wach, P., Chmura, L., Gorczyca, Z., Rozanski, K., Godlowska, J., Mazur, J., Kozak, K., Jericevic, A.: Factors controlling temporal variability of near-ground atmospheric ^{222}Rn concentration over central Europe. Atmos. Chem. Phys. 14, 9567-9581, doi: 10.5194/acp-14-9567-2014, 2014.~~